Composite Structures 327 (2024) 117663

Contents lists available at ScienceDirect

Composite Structures

journal homepage: www.elsevier.com/locate/compstruct

Review

Application of elastic metamaterials/meta-structures in civil engineering: A review

Nicolás Contreras [a], Xihong Zhang [a,*], Hong Hao [b,a], Francisco Hernández [c]

[a] Centre for Infrastructural Monitoring and Protection, School of Civil and Mechanical Engineering, Curtin University, Perth 6102, Australia
[b] Earthquake Engineering Research and Test Center, Guangzhou University, Guangzhou, China
[c] Faculty of Engineering and Applied Sciences, Universidad de los Andes, Chile

ARTICLE INFO

Keywords:
Metamaterial
Meta-concrete
Band gap
Wave attenuation

ABSTRACT

Inspired by sonic engineering, locally resonant metamaterials have attracted much attention from researchers in civil engineering for their unique characteristics of stress wave attenuation and vibration control capacities. This paper presents a comprehensive review of the latest progress of locally resonant metamaterials and their potential applications in civil engineering for structure protection against dynamic loads. The concepts of metamaterials for stress wave attenuation are introduced first, followed by a comprehensive overview of the historical origins and development of metamaterials. Existing analytical approaches for metamaterials, including theoretical solutions, numerical simulations, and experimental examinations, are summarised. Commonly used meta-structures with internal or external resonators and their applications are reviewed and discussed. Research gaps and future outlooks are also identified and briefed.

1. Introduction

Metamaterials are a novel technology that has recently attracted significant attention due to their novel applications, such as perfect lenses [1], invisibility cloak [2], and sound attenuation [3]. There is no consensus on the definition of metamaterials [4–6], but a broad description is that metamaterials are engineered functional materials or mechanisms that do not naturally exist. Civil engineering applications of metamaterials usually involve tremendous sizes and thus are not practical for common application [7] until the new millennium when locally resonant metamaterials emerged [8]; They exhibited excellent sonic wave attenuation properties without requiring impractical sizes [9]. It is commonly accepted that locally resonant metamaterials present negative effective linear elastic properties, enabling the attenuation of wave propagation within specific frequency ranges [10,11]. After their introduction, different locally resonant metamaterials emerged in the acoustic/elastic field [12–19]. In recent years, researchers in civil engineering have inherited the concept and discovered that by coating dense core materials with a soft shell before incorporating them into a host matrix, these materials could resonate and effectively attenuate the induced stress waves [20,21]. Different approaches, including theoretical derivation [22–24], numerical simulation [25], and experimental testing [26,27], have been employed to investigate metamaterial properties and develop targeted metamaterials for enhanced structural protection. Moreover, new characteristics, such as fluid-like behaviour [28], super-anisotropy [29], and asymmetric wave transmission [30,31], were discovered.

This paper reviews the latest research advancements in metamaterials, focusing on potential applications in civil engineering. It concentrates on metamaterials based on local resonance for wave energy trapping and conversion and their potential applications for structural protection against dynamic loads. There are seven sections in the paper. The 2nd section briefly overviews the history and evolution of metamaterials, tracing their origins in the electromagnetic field and exploring the critical concepts of resonances. The 3rd section reviews the approaches for predicting the band gap of metamaterials, followed by relevant working examples. The 4th and 5th sections present the recent progress of meta-structures with internal and externally attached locally resonant elements. The 6th section summarises methods for enhancing the band gaps for mitigating wave propagation. The last section concludes the paper and provides future outlooks.

* Corresponding author.
E-mail address: xihong.zhang@curtin.edu.au (X. Zhang).

https://doi.org/10.1016/j.compstruct.2023.117663
Received 6 June 2023; Received in revised form 14 August 2023; Accepted 26 October 2023
Available online 28 October 2023

2. History

2.1. From optics to acoustics

Studies on metamaterials date back to ancient Rome, where dichroic glasses emerged hundreds of years before the term "metamaterials" was coined [2]. An example of dichroic glasses is the Lycurgus cup, made of a silver-gold alloy [32]. Barber and Freestone [32] discovered that silver produced a green colour under reflected light waves, and gold created a red colour when the glass is under transmitted light. Researchers recognize Bose [33] and Rayleigh [34] as the pioneers who first ventured into metamaterials in modern science [35,36], while Veselago was the first to attempt the development of electromagnetic metamaterials [37–41]. Veselago [42] theoretically discussed particular effects (namely reversed Doppler effect and the reversed Vavilov-Cerenkov effect), which emerge when the dielectric constant and magnetic permeability are negative.

In 1987, Yablonovitch [43] designed a three-dimensional crystal growth with a face-centred-cubic reciprocal lattice to reduce the spontaneous emission in the electromagnetic band gap. This idea began with photonic crystals, a name derived from their connection to crystallography [7]. Sigalas and Economou [3] adapted photonic crystals as phononic crystals. They studied a type of phononic crystal composed of a homogeneous medium embedded with identical spheres arranged using different crystal systems. Particular frequency ranges emerged in which elastic and acoustic waves could not propagate, which was thus named "band gap" [3]. In 1995, Martínez-Sala et al. [44] experimentally demonstrated the effect of phononic crystals. They designed an acoustic sculpture composed of a periodic array of hollow stainless cylinders with simple cubic symmetry. This arrangement exhibited attenuation caused by Bragg scattering between the hollow tubes, where the tubes were spaced periodically at a distance of half the wavelength of the targeted wave. This spacing produced an absorption and radiation pattern that negatively interfered with the wave propagation.

At the turn of the millennium, new concepts of metamaterials began to emerge and were subsequently validated through experimental testing. In the electromagnetic field, Smith et al. [45] experimentally observed that a periodic system composed of several split ring resonators could exhibit a negative magnetic permeability around its resonance peaks. They combined the split ring resonators with a negative effective dielectric constant material to create a left-handed substance. In the same year, Pendry [1] proposed super-lenses capable of amplifying transmitted evanescent waves, enhancing the image resolution beyond the wavelength limitation. Later, Shelby et al. [46] experimentally demonstrated new left-handed applications, including filters, modulators, and beam steerers.

In the acoustic field, Liu et al. [8] constructed a cubical structure using an epoxy matrix embedded with 8 x 8 x 8 silicone-coated lead balls. Despite the lattice order being two orders lower than the wavelength of the incident wave, the crystal attenuated sonic waves. Moreover, the authors distinguished two main transmission dips. They concluded that the first dip resulted from the resonance of the lead balls within the soft coating, while the resonance of the coating caused the second dip. This study originated the locally resonant metamaterials and developed a new method to attenuate waves that do not depend on Bragg scattering [5].

2.2. Classification of metamaterials

Metamaterials constitute a multidisciplinary subject encompassing electromagnetic, optical, acoustic, and mechanical metamaterials [6,39,47]. Microscopic and complex geometrical materials are commonly defined as mechanical metamaterials [48–50]. Some authors treated acoustic metamaterials as a specific type of mechanical metamaterials [35], while others employed terms like elastic or elastic/acoustic metamaterials to describe stress and acoustic waves travelling through solids [19,51].

This paper introduces a novel metamaterial classification tailored for civil engineering applications based on the specific types of waves targeted for mitigation. In Fig. 1, metamaterials are classified according to their target wave types, providing a visual representation of the categorization. Electromagnetic metamaterials and photonic crystals aim to modify electromagnetic waves, deriving their distinctive properties from incorporating negative magnetic permeability, negative dielectric constant, and Bragg scattering, respectively [13]. Conversely, mechanical metamaterials focus on mitigating mechanical waves, exhibiting negative equivalent linear elastic properties such as negative mass, negative bulk modulus/ modulus of rigidity, negative elasticity modulus, and negative Poisson's ratio [35,47]. Additionally, mechanical metamaterials encompass acoustic/elastic metamaterials, which can be classified based on their capacity to attenuate sound or stress waves. When the underlying mechanism for attenuation is Bragg scattering, these systems are termed phononic crystals or structures [7]. Conversely, when the attenuation results from locally resonant elements, the systems fall under acoustic or stress metamaterials. Stress metamaterials can be further sub-categorized into load-bearing structures with embedded resonating (meta-structures with internal resonators) and structures with external resonating elements.

2.3. Negative effective linear elastic properties through local resonances

One of the main concepts behind sonic locally resonant elements is that resonances in the system can produce negative effective linear elastic properties. Sheng et al. [10] discovered sound wave attenuation capabilities in a circular epoxy slab with rubberized metallic cores. The material displayed two partial band gaps attributed to negative effective linear elastic properties. Modal shapes corresponding to the translational movements of the core and coating deformation generated the band gaps [9]. However, Core rotational modes did not contribute forces or produce band gaps [61,62].

Studies detected negative effective linear elastic properties years before the advent of locally resonant elements. Berryman [63] proposed an expression to estimate the effective macroscopic linear elastic constant for heterogeneous materials, yielding an expression for the effective mass density different from the intuitive volume-averaged mass density. Likewise, Mei et al. [11] expanded Berryman's expression for a hybrid system with a high-density difference between the matrix and the core materials. As a result, an effective negative mass density [11], negative bulk modulus [12], and negative shear modulus [14] emerged when local resonance occurred in the system. Chan and co-workers [13] suggested that negative mass density can be observed when the system is excited near the resonance frequency of the core due to an out-of-phase movement (axial translational resonance) between the matrix and the core.

Besides the axial translational resonance, Liu et al. [64] proposed using a chiral coating to induce rotational resonance. The asymmetry of the chiral coating resulted in the rotational movement of the core, leading to an expansion of the unit cell and a negative effective bulk modulus [65]. Another resonance is the axial-lateral translational resonance, which leads to an effective negative modulus in the system [66]. A detailed explanation of the resonance is provided in Section 3.2. Finally, Zhou et al. [67] observed coating resonance due to a differential prolate shape deformation between the matrix and the coating. Consequently, when a stress wave travels through the system, the matrix compresses in the vertical direction and expands in the lateral direction resulting in a negative shear modulus.

3. Prediction of band gap for stress metamaterials

Stress metamaterials possess the distinctive ability to attenuate stress waves within a band gap [68]. Predicting the band gap is not straightforward. Some researchers have employed numerical simulation

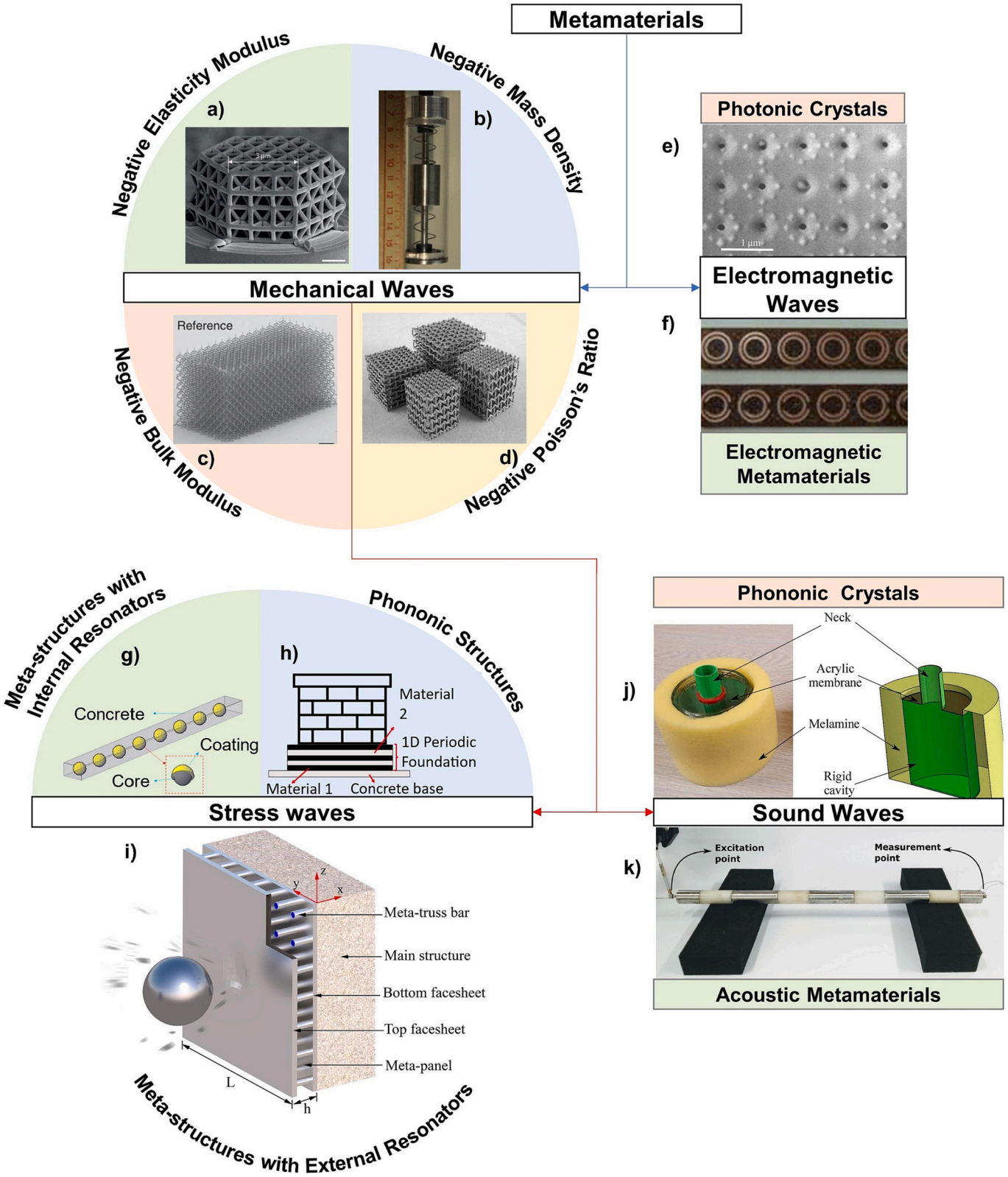

Fig. 1. Classification of metamaterials: a) 3-D printed polymeric micro-lattices. Copyright 2016, Springer Nature [52]; b) Spring-mass single resonator. Copyright 2023, Elsevier [53]; c) Electron micrograph of a homogeneous pentamode metamaterial. Copyright 2014, Springer Nature [54]; d) Image of an auxetic metamaterial captured by the Arcam EBM machine. Copyright 2015, Elsevier [55]; e) Scanning electron microscopy image of a photonic crystal with embedded emitters (Ge/Si QDs). Copyright 2023, Elsevier [56]; f) Split-ring resonators. CC BY 4.0 [57]; g) Schematization of a meta-concrete bar; h) Schematization of a periodic foundation; i) Schematization of a meta-panel used as a protective element. Copyright 2022, Elsevier [58]; j) Membrane-cavity Helmholtz resonator. Copyright 2019, Elsevier [59]; k) Experimental setup of a phononic crystal composed of successive layers of steel and polyacetal (white). Copyright 2020, Elsevier [60].

approaches using commercial software, such as Abaqus ([51,68]) or COMSOL multi-physics ([69,70]), to calculate band gaps and evaluate methods of control. Others have utilised theoretical methods, including the Hamilton principle [71], vibration theory [24], and a mix of Bloch theory with the spectral method [72–78]. While these different methods have offered essential insights into the band gap limits and attenuation capacity, they also require a high computational time. In contrast, studies have demonstrated that the theoretical spring-mass method is more intuitive for predicting the band gap and attenuation levels of stress metamaterials [5,20,22,23,79]. This section summarises the fundamental studies that led to the expressions for predicting band gaps of stress metamaterials based on the spring-mass method. Their advantages and disadvantages are discussed.

3.1. Metamaterials with axial translational resonances

The derivation of theoretical solutions for determining band gaps in stress metamaterials was closely linked with the progression of acoustic metamaterials. From its origins, scholars developed different theoretical methods to investigate the sonic wave attenuation mechanism, including the multiple scattering theory [8], the lumped mass method [73], the variational method [75], and the plane-wave expansion method [7]. For instance, Goffaux et al. [80] and Chan et al. [13] delved into the simplification of analyzing acoustic metamaterials with axial translational resonances by representing them as one-dimensional spring-mass systems. The utilization of a one-dimensional spring-mass system to simplify stress metamaterials with axial translational resonances was pioneered by Milton and Willis [79]. Fig. 2a illustrates the nomenclature used for the components of the mass-in-mass lattice system: the "matrix" for the host material, the "core" for the resonating element, and the "coating" for the soft material covering the resonating element. The representation of cores and matrix employs lumped masses connected with springs. Masses m_1 represent the matrix mass; masses m_2 symbolise the resonator mass; springs k_{a1} represent the matrix axial stiffness; springs k_{a2} symbolise the coating axial stiffness; and k_{s1} and k_{s2} are the corresponding shear stiffness. Using the simplified spring-mass system, Chan et al. [13] and Milton and Willis [79] derived Eqs. (1) and (2) to express the response of the metamaterials under the excitation of stress waves, respectively. The studies concluded that the vibrating mass of a metamaterial was sensitive to the frequency of the applied load, resulting in an effective linear elastic property, the effective mass (m_{eff}). The research revealed that the effective mass could become negative, producing a band gap and attenuating the propagated stress wave within a specific frequency range.

Nevertheless, the simplified spring-mass system described by Eqs. (1) and (2) showed to be incomplete. Huang et al. [23] noted that the effective mass resulted from the homogenisation of the system and that the dispersion relation, which relates the wave spatial frequency (i.e., wave number) to the wave frequency, captured the true response. They further noted that the imaginary part of the dispersion relation represented the spatial decay associated with the band gap [23]. Liu et al. [5,20] also found that the axial and shear responses of the coating could influence the band gap of a metamaterial. To address the coating, they introduced a new effective linear elastic parameter called effective stiffness (k_{eff}) [20]. Additionally, they concluded that the effective mass and stiffness combined response resulted in the same band gap as the dispersion relation [20]. Moreover, Liu et al. [5] highlighted that the shear stiffness of the matrix could also impact the band gap. Vo et al. [22] recently enhanced the previous analysis by proposing the spring-mass system of Fig. 2b, the dispersion relation of Eq. (3), and the effective linear elastic parameters of Eq. (4)-(5).

$$m_{eff} = m_1 + \frac{m_2\omega_{0atr}^2}{\omega_{0atr}^2 - \omega^2} \tag{1}$$

$$m_{eff} = M_1\left(1 + \frac{nm_2\omega_{0atr}^2}{M_1(\omega_{0atr}^2 - \omega^2)}\right) \tag{2}$$

$$\cos(ql) = 1 - \frac{m_1\omega^2 - (k_{s1} + k_{a2}) + \frac{k_{a2}^2/m_2}{\omega_{0atr}^2 - \omega^2}}{2k_{a1}} \tag{3}$$

$$m_{eff} = m_1 + \left[\frac{k_{a2}^2/m_2}{\omega_{0atr}^2 - \omega^2} - (k_{s1} + k_{a2})\right]\frac{1}{\omega^2} \tag{4}$$

$$k_{eff} = k_{a1} + \frac{1}{4}(k_{s1} + k_{a2}) - \frac{1}{4}\left(m_1\omega^2 + \frac{k_{a2}^2/m_2}{\omega_{0atr}^2 - \omega^2}\right) \tag{5}$$

where: $\omega_{0atr} = \sqrt{k_{a2}/m_2}$ - Natural angular frequency of the axial translational resonance; ω: Forcing angular frequency; M_1: Total matrix mass; n: Resonator number; q: Wave spatial frequency; l : Distance between m_1; ql : Wave number.

Predicting a band gap using the spring-mass method is only valid when there is a perfect energy transfer between the core and the coating and when the system is infinite, elastic, one-dimensional, and periodic. Some authors examined the suitability of the assumptions. Mitchel et al. [68] observed that the perfect energy transfer assumption might not always hold, especially when the coating is excessively soft or hard compared to the matrix and the core. In scenarios involving blast and impact loading, the presumption of linear-elastic behaviour in metamaterials was not valid [81]. Furthermore, in non-periodic systems, the upper limit of the predicted band gap shifted [27,82]. Last but not least, the predicted band gap limits were only accurate when the system included an infinite or a sufficient number of cores [82]. Experimental tests have also examined the prediction accuracy for band gaps. For example, Briccola and Pandolfi [27] conducted a non-destructive

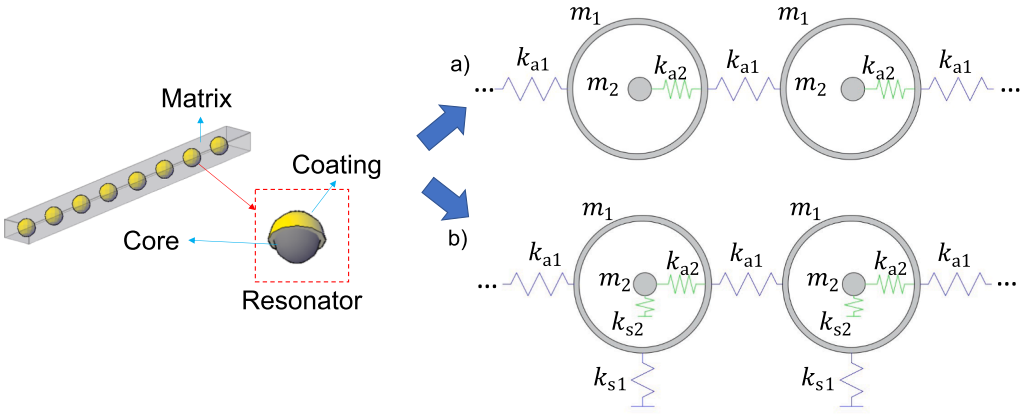

Fig. 2. Simplification of a metamaterial to a mass-in-mass lattice system: (a) without shear stiffness and (b) with shear stiffness.

dynamic test on a meta-concrete cylinder, where the band gap emerged in the predicted frequencies of the dispersion relation. Similar validation tests were also conducted on beams with attached spring-mass systems [82], meta-trusses [26], spring-mass systems [83,84], and sonic locally resonant elements [8].

3.2. Metamaterials with axial-lateral translational resonance

In parallel to systems with translational resonances, some research [66,85,86] extended the concept of Helmholtz resonators [87] to elastic metamaterials, resulting in axial-lateral translational resonance. Helmholtz resonators are known for producing a negative effective bulk modulus [40,88]. When mixed with a system with negative effective mass, passbands appeared at the frequencies where the effective linear elastic properties overlapped. Huang and Sun [66] introduced an "elastic Helmholtz resonator", depicted in Fig. 3. Lumped masses m_1 and springs k_{a1} represent the matrix mass and uniaxial stiffness, respectively. The resonating element is constituted by a spring-mass system (k_{l2}, m_2) connected to the matrix through two rigid trusses. This configuration yielded a band gap with a negative effective modulus of the elastic solid, which can be predicted with Eq. (6)-(12).

$$\eta^4 - \left(1 + 2\left(\frac{\theta}{\delta_{lt}} + \frac{\theta\mu}{2}\right)(1 - \cos(ql))\right)\eta^2 + 2\frac{\theta}{\delta}(1 - \cos(ql)) = 0 \tag{6}$$

$$\theta = \frac{m_2}{m_1} \tag{7}$$

$$\frac{E_{eff}}{E_1} = 1 + \frac{\delta_{lt}\mu\eta^2}{2(\eta^2 - 1)} \tag{8}$$

$$\mu = \left(\frac{l}{D}\right)^2 \tag{9}$$

$$\delta_{lt} = \frac{k_{l2}}{k_{a1}} \tag{10}$$

$$E_1 = k_{a1} l / A \tag{11}$$

$$\eta = \frac{\omega}{\omega_{0atlr}} \tag{12}$$

where: η: Non-dimensional wave frequency; θ: Mass ratio; δ_{lt}: Stiffness ratio of the axial-lateral translational resonance lattice system; μ: Geometry ratio of the axial-lateral translational resonance lattice system; E_{eff}: Effective modulus of the elastic solid; E_1: Matrix static elasticity modulus; D : Vertical distance of the rigid element. A : Elastic solid cross-section; k_{l2}: Coating axial-lateral stiffness; $\omega_{0atlr} = \sqrt{k_{l2}/m_2}$- Natural angular frequency of the axial-lateral translational resonance.

3.3. Metamaterials with rotational resonance

Rotational resonances exist naturally in metamaterials. However, they are generally hard to excite [9,61,62]. Liu et al. [64] used chirality [50,89] to excite metamaterial, where the green ligaments in Fig. 4a modified the coating. The ligaments generated an asymmetry in the system enabling core rotation under compressive loading [65]. Due to the complex geometry of the resonances, ad hoc theoretical models should simplify each geometry. Nonetheless, following the spirit of the previous sections, a simplified system is presented. Liu and Hu [17] derived theoretical expressions for the dispersion relation (Eq. (13)), k_{eff} (Eq. (14)) and m_{eff} (Eq. (16)). Fig. 4b illustrates the variables of the equations. Numerical simulation [64] and experimental testing [90] proved that the rotational resonances yielded a wave attenuation. Studies did not compare the predicted band gap with the testing results. In general, metamaterials with rotational resonances are typically complex and thus challenging to construct, which therefore have not been commonly used.

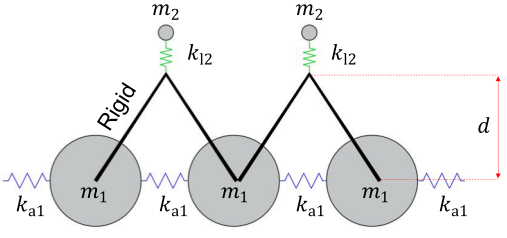

Fig. 3. Axial-lateral translational resonance lattice system.

$$\omega^2\left(m_1 + \frac{m_2\omega_{0ar}^2}{\omega_{0ar}^2 - \omega^2}\right) = \left[k_{a1} + \frac{k_{r2}\cos^2\alpha}{2}\left(\frac{\omega_{0ar}^2}{\omega_{0ar}^2 - \omega^2} - \frac{\omega_{0rr}^2}{\omega_{0rr}^2 - \omega^2}\right)\right]\sin^2(0.5ql) \tag{13}$$

$$k_{eff} = k_{a1} - \frac{m_1}{4}\omega^2 + \frac{k_{r2}\cos^2(\alpha)\omega^2}{2(\omega^2 - \omega_{0rr}^2)} \tag{14}$$

$$\omega_{0ar}^2 = \frac{2k_{r2}\cos^2\alpha}{m_2} \tag{15}$$

$$m_{eff} = m_1 + \frac{m_2\omega_{0ar}^2}{\omega_{0ar}^2 - \omega^2} \tag{16}$$

$$\omega_{0rr}^2 = \frac{2k_{r2}r_2^2}{I_2} \tag{17}$$

where: ω_{0ar}: Axial natural angular frequency of m_2; k_{r2}: Coating rotational stiffness. α: k_{r2} inclination angle; ω_{0rr}: Rotational natural angular frequency of m_2; r_2: Core radius; I_2: Core Inertia.

3.4. Working example for prediction of the band gap for metamaterials

To provide readers with insights into band gaps, expected attenuation levels, and phenomena arising from the resonances, the spring-mass methods, summarised in Sections 3.1, 3.2, and 3.3, were compared. Four cases were examined: (1) a system with axial translational resonance without considering the material shear stiffness; (2) a system with axial translational resonance considering the material shear stiffness; (3) a system with axial and lateral translational resonance; and (4) a system with rotational and axial translational resonance. For unified comparisons, the parameters of Table 1 were used. The natural frequency was maintained ($\omega_0 = 1$ rad), while the mass ratio θ and stiffness ratio Δ were varied case by case.

Following [20], band gaps of a metamaterial were detected at the frequencies where the effective linear elastic properties (m_{eff} and k_{eff}) become negative. Moreover, the non-zero values of the imaginary part in the dispersion relation (Imag(ql)) set the boundaries of the band gap and define the spatial decay of the system [23]. Fig. 5 shows the predicted band gaps using the negative effective linear elastic properties and the imaginary part of the dispersion relation. The dispersion relation was obtained using Eq.(3) for cases 1 and 2, Eq. (6) for case 3 and Eq. (13) for case 4. In the figure, the dispersion relation, the effective mass, and the effective stiffness were highlighted in pink, green, and purple, respectively. Table 1 shows the values of band gaps.

As shown in Fig. 5a, the dispersion relation of Case 1 displayed two band gaps, i.e., one around ω_0 of the translational resonance (BG1) and the other in higher frequencies (BG2). By complementing the previous results with the effective linear elastic parameters, it is noted that BG1 was formed by the combination of m_{eff} and k_{eff}, and BG2 was formed by k_{eff}. The dispersion relation of Fig. 5b shows a new band gap (BG0) with the peculiarity of starting from 0 Hz; it is noted that the m_{eff} formed this new band gap. Furthermore, it is observed in Fig. 5c that BG1 was

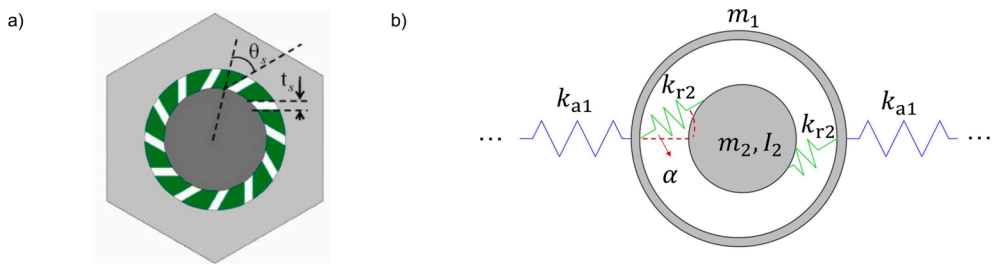

Fig. 4. A) unit cell of a rotational resonance mass-in-mass lattice system. copyright 2011, aip publishing [65]; b) Chain of a rotational resonance mass-in-mass lattice system.

Table 1
Parameters and results of theoretical analysis. $\omega_0 = \omega_{0atr}$ for cases 1 and 2; $\omega_0 = \omega_{0atlr}$ for case 3; $\omega_0 = \omega_{0rr}$ for case 4. $\Delta = k_{a2}/k_{a1}$ for cases 1 and 2. $\Delta = \delta_{lt}$ for case 3. $\Delta = k_{r2}/k_{a1}$ for case 4.

Case	ω_0[rad]	ω_{0ar}[rad]	Δ[-]	θ[-]	η[-]	I_2[kg*m^2]	Band gap Imag(ql) [-]	Band gap m_{eff}/m_1[-]	Band gap $k_{eff\ f}/E_{eff}$ [-]
1	1	–	0.9	0.9	–	–	0.9–1.4;2.3–3	1–1.4	0.9–1;2.3–3
2	1	–	0.9	0.9	0.5	–	0–0.5;0.9–1.5;2.4–3	0–0.5;1–1.5	0.9–1;2.4–3
3	1	–	0.9	0.9	–	–	0.8–1;2.5–3		0.8–1
4	1	1	0.8	1.2	–	0.0038	1–1.3;1.5–1.6;2.5–3	1–1.5	1.3–1.6;2.5–3

formed by the effective modulus of the elastic solid with a frequency range below ω_0. In addition, the dispersion relation of Fig. 5d depicts the formation of three band gaps whose origins can be explained by the effective linear elastic properties. The k_{eff} opened the highest frequency band gap, similar to cases 1 and 2. The effective mass and stiffness displayed a gap where they overlapped. The gap generated a passband in the dispersion relation, which divided the band gap into two segments. Thus, the effective mass formed the lowest frequency band gap, and the effective stiffness created the medium-frequency band gap.

As seen above, the locations of the band gaps were highly dependent on the natural frequency of the resonance. The natural frequencies of locally resonant elements in the literature showed that producing a system with low natural frequencies was challenging because of the core weight required, the sizes of the structures and the available construction space [10,20,91,92]. Even seismic metamaterials (to be elaborated in Section 5.2), which use more extensive elements, struggled to generate low-frequency band gaps [93–95]. Therefore, Cases 1, 3, and 4 were primarily designed to attenuate impact and blast loads [51,68,96,97]. However, low-frequency band gaps are still desirable for attenuating seismic waves and improving the efficiency of metamaterials against impact and blast loads. Case 3 could be an option to produce low-frequency band gaps. Nonetheless, the band gap is narrower than that in the other cases. Thus, the efficiency should be further studied. Case 2 presents a viable solution for attenuating stress waves with low frequency. It involves encasing the matrix or coating with a stiff outer element (explained in Section 5.1), considering the shear resistance and deformation of the coated material. It is noted that this deformation may be high and consequently unsuitable for structures, necessitating additional research for a thorough evaluation.

3.5. Numerical simulation methods for detecting band gaps

Numerical simulations were also employed to detect band gaps of stress metamaterials, primarily including the following methods: Finite Element Modal Analysis (FEMA) [69,98,99], Band Structure Analysis (BSA) [69,100], Effective Mass Analysis (EMA) [69,92,100], and Transmission Spectrum Analysis (TSA) [5,20,22,51,69,96,98,101,102]. The first three methods focus on a unit cell, while the fourth explores a chain of unit cells. FEMA focuses on modelling a unit cell to determine its natural frequencies, which can detect the natural resonances of the core and coating in elastic metamaterials with complex geometries [8]. However, the FEMA method requires fixed boundary conditions, which thus omits natural frequencies associated with asynchronous core-coating movements [9,98]. Previous study on hammer impact tests showed discrepancies between experimentally detected natural frequencies and that predicted by the FEMA method [99].

BSA [69,100] models a unit cell with periodic boundary conditions, studying eigenvalues inside the first irreducible Brillouin zone and establishing the dispersion relation. The EMA proposed by Ma et al. [69] employs a numerical model of a periodic unit cell to obtain F_i^{eff}, u_i^{eff}, and various mode shapes. It then employs equation (18) to determine the relation between effective mass density (ρ^{eff}) and natural frequencies. The EMA is helpful in analysing changes in the band gap resulting from variations in core and coating properties and core and coating volume compared with the matrix volume. BSA and EMA could provide band gap limits compared to the FEMA method. A previous study revealed similar band gaps predicted using the BSA and EMA methods compared to laboratory testing data [69].

$$\rho_i^{eff} = \frac{-F_i^{eff}}{\omega_{nf}^2 u_i^{eff} a^3} \tag{18}$$

where: ρ_i^{eff}: effective mass density in the analysis direction i; F_i^{eff} : Effective net force exerted on the unit cell in the analysis direction i; u_i^{eff} : Effective net displacement of the unit cell in the analysis direction i; a: Unit cell length. ω_{nf}: Natural angular frequency.

TSA models a metamaterial using a continuum model [98] or a spring-mass lattice system [51]. The imposed harmonic [20], impact, or blast load [51] propagates through the chain, where the interaction between the wave and the cores can be analysed. Previous studies evaluated the wave amplitudes of input and output waves [20,69,96,102] and the energy in the last core and all cores [98]. Frequency domain analysis can be performed to identify band gaps as dips that correspond to the natural frequencies of the resonators. A previous TSA method study found that more cores could enhance wave attenuation through the band gaps [5]. Larger core sizes widened the band gap while increasing coating thickness and core density lowered the band gap frequencies. Increasing coating stiffness beyond a certain threshold also raised the band gap frequencies [102]. Some laboratory validation tests found that the TSA method could yield good predictions of band gaps [22,69,101]. In contrast, others reported narrower band gaps using the TSA method than those from their laboratory test data [101].

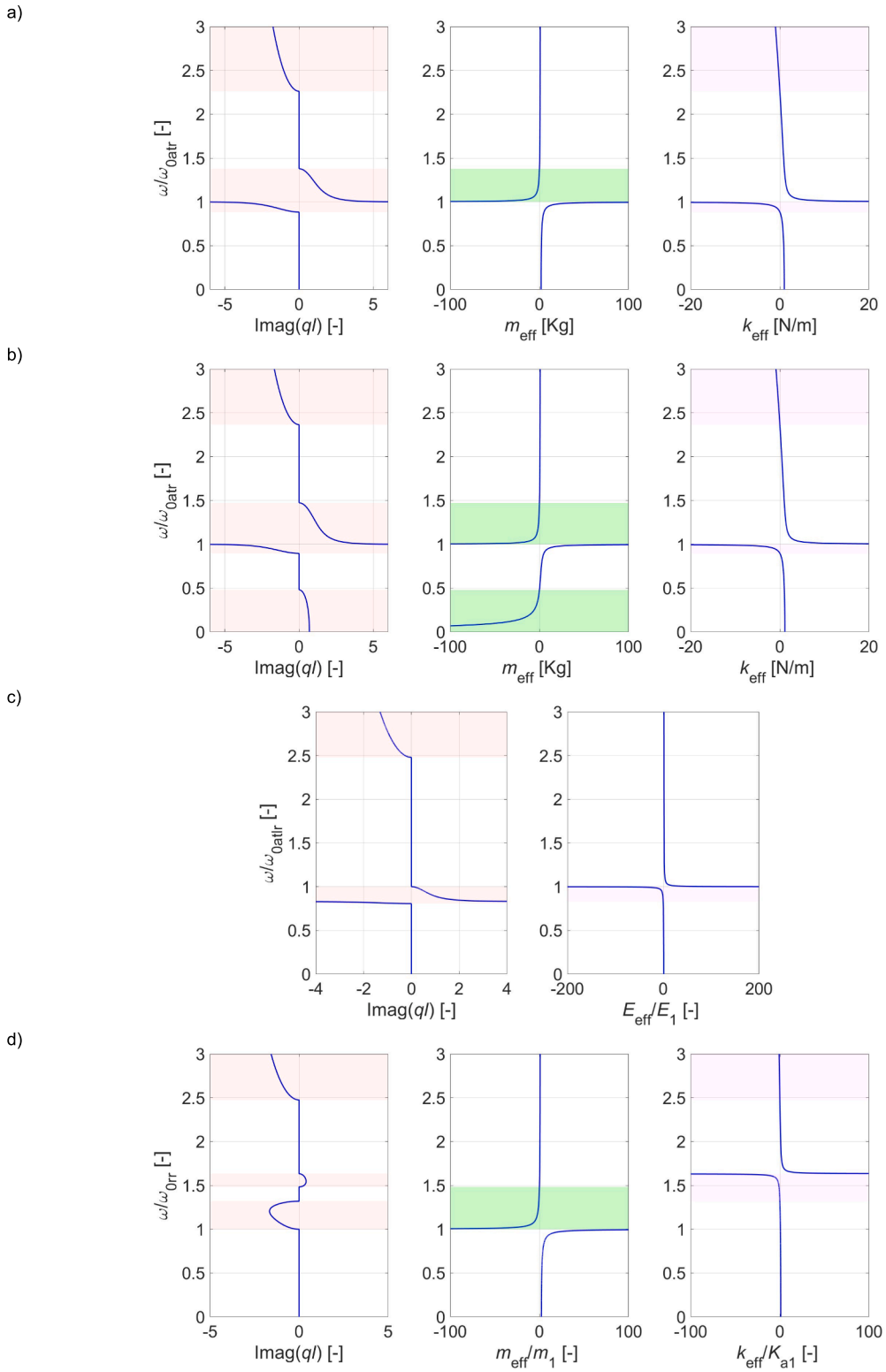

Fig. 5. Dispersion relations and effective linear elastic parameters of examples: a) Case 1; b) Case 2; c) Case 3, and d) Case 4. Pink areas indicate regions where the imaginary part of the dispersion relation is non-zero. Green areas represent regions with negative effective mass. Purple areas denote regions with negative effective stiffness. (For interpretation of the references to colour in this figure legend, the reader is referred to the web version of this article.)

Studies compared band gaps obtained by different numerical simulation methods. Generally, FEMA-predicted natural frequencies were within TSA-predicted band gaps [69,98]. In some cases, the natural frequency was at the beginning of the band gap [98], while in others, it was at the end [69]. BSA and EMA were also used to predict band gaps, showing good agreement in their comparison [100]. TSA-predicted band gaps were also compared to those from BSA and EMA, yielding similar results [69]. Furthermore, studies compared numerically predicted with spring-mass predicted band gap. EMA indicated that the band gap depends not only on mass core and coating stiffness (as in

equation (3)) but also on the coating Poisson's ratio, core volume to the matrix cell volume, and stiffness difference between the matrix and the coating. TSA compared its prediction of BG1 and BG2 with equation (3), revealing that BG2 was not infinite in the high-frequency range as predicted by the equation. Increasing the core number led to wider band gaps than equation (1) [51]. Comparing the predicted ultra-low frequency band gap by TSA and equation (3) showed good results [20]. However, FEMA demonstrated that obtaining the natural frequency through equation (1) could underestimate the value [98].

4. Structures with internal resonators

Locally resonant metamaterials with axial translational resonances have diverse applications in civil engineering, which are classified into structures with internal and external resonators in this review. As defined, in the former type, the resonators are an inherent part of the material, while in the latter category, the resonators are positioned externally to safeguard the main structure. Structures with external resonators offer the advantage of protecting existing and new structures while facilitating ease of repair. However, this approach necessitates additional construction space and resources beyond the main structure. Conversely, structures with internal resonators do not require extra space, as the resonators are an integral part of the structure. Nevertheless, they are limited to new structures and entail higher replacement costs if damaged.

This section reviews meta-structures with internal resonators, specifically delving into the energy-storing mechanism and meta-concrete concept. On the other hand, Section 5 reviews meta-structures with external resonators.

4.1. Energy storing mechanism

Although the dispersion relation predicts the band gap location and the magnitude of the expected attenuation, it cannot directly elucidate the energy-storing mechanisms. To comprehend the response of a locally resonant element with translational resonances, Fig. 6 illustrates the three primary responses of locally resonant elements, as described in the literature, namely: core resonance, energy storage in the resonating elements, and the reflection of energy associated with the band gap [51,66,103,104]. The figure depicts a mass-in-mass lattice system consisting of a long chain of meta-units (medium II) sandwiched between non-meta-units (medium I and III). When a load with a frequency content within the band gap of the resonators interacts with the system, the locally resonant elements react, transform and absorb the imposed energy into kinetic energy. Subsequently, the absorbed energy returns to the system relatively slowly compared to the applied wave. The released energy then propagates to mediums I and III. However, in cases where the chain is sufficiently long, a not significant portion of the stored energy reaches medium III, concluding that the meta-medium reflects the imposed wave.

Locally resonant metamaterials presented other interesting mechanisms. Materials with double negative parameters showed a negative phase velocity [85]. Systems with two types of meta-units exhibited two band gaps [51,105]. Furthermore, meta-units displayed anisotropic properties, which enables the manipulation of wave propagation direction [20]. Moreover, the anisotropic character could generate a fluid-like behaviour [68], i.e., band gaps permit shear-only or compression-only waves to propagate [28,29]. Xiao et al. [72] also observed Bragg scattering in combination with mass-in-mass lattice systems.

Mass-in-mass lattice systems suffer inherited difficulties in adequately explaining the energy-storing mechanism in metamaterials. This is because, in theory, the meta-medium could attenuate the transit of wave frequencies within the band gap [82]; however, in reality, waves still propagate through the meta-medium [53,106]. Metamaterials are finite, violating the assumption of the mass-in-mass lattice system. Studies quantified the influence of unit cell number in

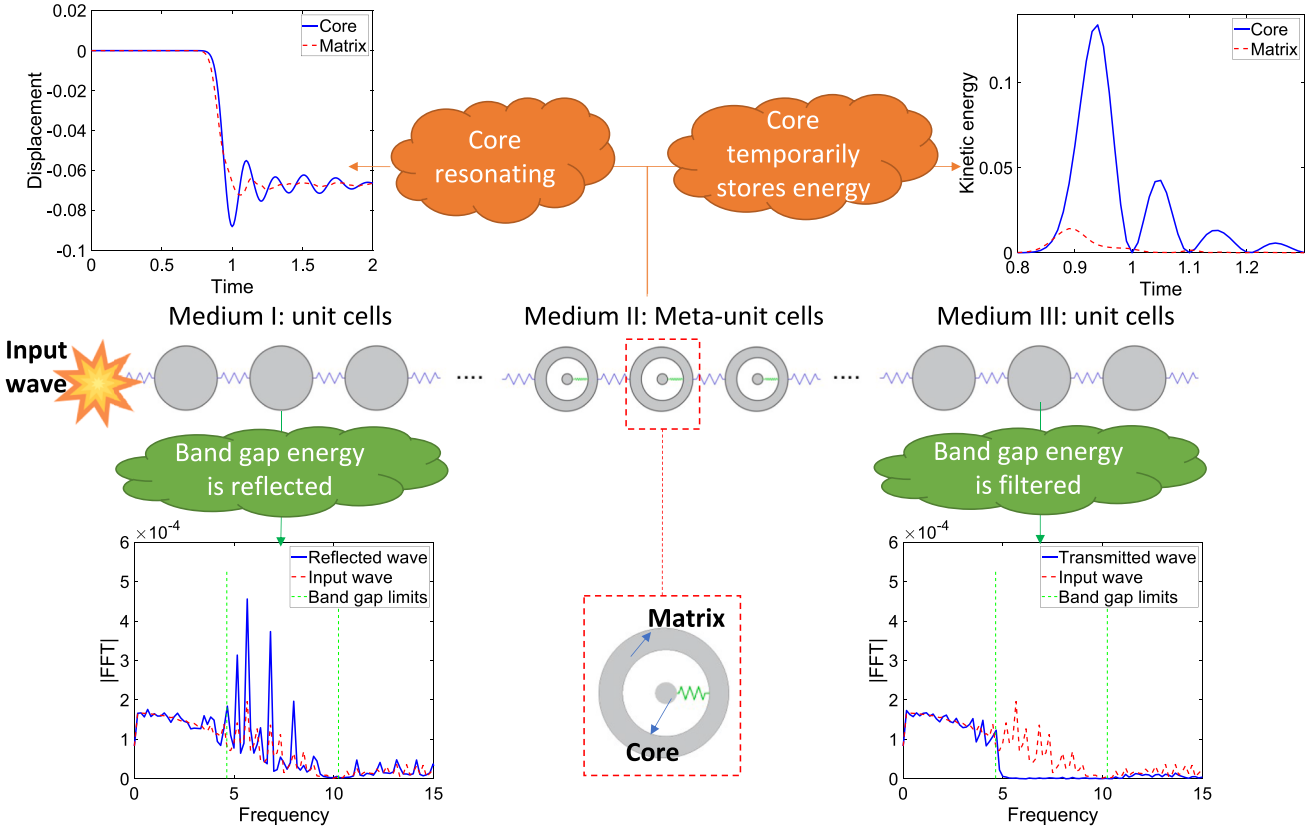

Fig. 6. Main mechanisms displayed by locally resonant elements.

metamaterials [107]. Researchers embedded an encased spring-mass system into a mortar cube and subjected it to dynamic vibration. The study observed that utilizing five meta-unit cells decreased the input acceleration to 90 % while employing ten meta-unit cells reduced the input acceleration to 98 % [107]. Surprisingly, increasing the meta-units did not yield a proportional increase in the attenuated energy [53,107]. Several factors could explain this observation, including the asynchronous movement of meta-units [82], the damping of the material reducing the attenuation peaks [108], or the wave propagation through the matrix [58]. Furthermore, the activation of meta-units depends on the location of the band gap at the high-energy zones of the incoming wave [106]. Thus, determining an optimized number of unit cells remains a challenge.

Regarding the design of unit cells, the ratio of core over matrix mass is demonstrated to be the most relevant parameter to control the bandwidth [51,72,105,109]. Several designs of unit cells emerged in the acoustic [36,87,110–112] and elastic fields [18,28,66,113–120]. Fig. 7 illustrates some designs of unit cells for civil engineering applications, such as the encased spring-mass system [107], the meta-beam system [121], the meta-lattice truss system [26], the tip-loaded cantilever beam resonator system [53], and the meta-bar system [69]. Encased-spring mass systems stand out among these systems because they are easy to build (Fig. 7d). Testing exhibited a clear out-of-phase motion [83,84] and improved response reduction against impact loadings [106,107]. Also, the tip-loaded cantilever beam resonator (Fig. 7a) and meta-beam systems (Fig. 7b) exhibited excellent vibration control capacities [53]. The meta-lattice truss system (Fig. 7c) underwent testing recently under impact loading, demonstrating exceptional performance [26]. In addition, several studies evaluated the performance and characteristics of the meta-bar system, which revealed noticeable energy dissipation performance [68,69,96].

4.2. Meta-concrete

Mitchel et al. [68] devised meta-concrete by substituting conventional gravels with axial translational coated cores, creating a meta-structure with internal resonators. Since then, many studies have focused on meta-concrete because of its superior performance under impact and blast loadings. One of the critical points of meta-concrete is how to design the cores to store the maximum amount of energy to protect a structure. Numerical simulation [68,102,123] found that a more efficient energy transfer between the core and matrix can be achieved when the coating stiffness is comparable to the stiffness of the core and the matrix. However, the coating must also be soft enough to allow the core to vibrate. Moreover, increasing the density [102,123] and the number of cores [98] expanded the core energy storage. The band gap performance improved when the cores covered the frequency range corresponding to the higher energy imposed by the load [102].

Fig. 8a and b display numerical simulations of two meta-concrete bars subjected to impulsive loads [102]. The simulations involved four locally resonant elements constructed with metal spheres coated by a soft layer, each with a different band gap. Model M-CB3 comprised eight identical coated cores to achieve a single band gap, while model M-GEA included eight coated cores with four different sphere types, resulting in four distinct band gaps. Fig. 8c illustrates the wave attenuation mechanism of the models before (0.1 ms) and after wave reflection (0.5 ms). The existence of coated cores effectively decreased the longitudinal stress, but the simulation results showed plastic strain concentration around the cores. Model M-CB3 displayed concentrations at the beginning and the protected zone. Similarly, model M-GEA also showed the plastic strain concentration at the left side of the bar where the impact load was applied. However, the concentration around the cores was lower than model M-CB3 [102]. In summary, both models showed stress wave attenuation, protecting the bar structure. Nevertheless, both developed stress concentrations and, thus, severe damage to the specimens.

The previous models exhibited two responses of the meta-concrete, i.e., the band gaps formed by the combinations of multi-types of cores, which successfully filtered the wave (model M-GEA) in the structure, and the band gaps from the single type of cores, which were not wide enough to filter out stress waves for structure protections (Model M-CB3). Studies complemented the first case by investigating the effect of erosion in the system [81]. The cores effectively reduced the wave, preventing spalling damage after the wave reflection. Furthermore, the

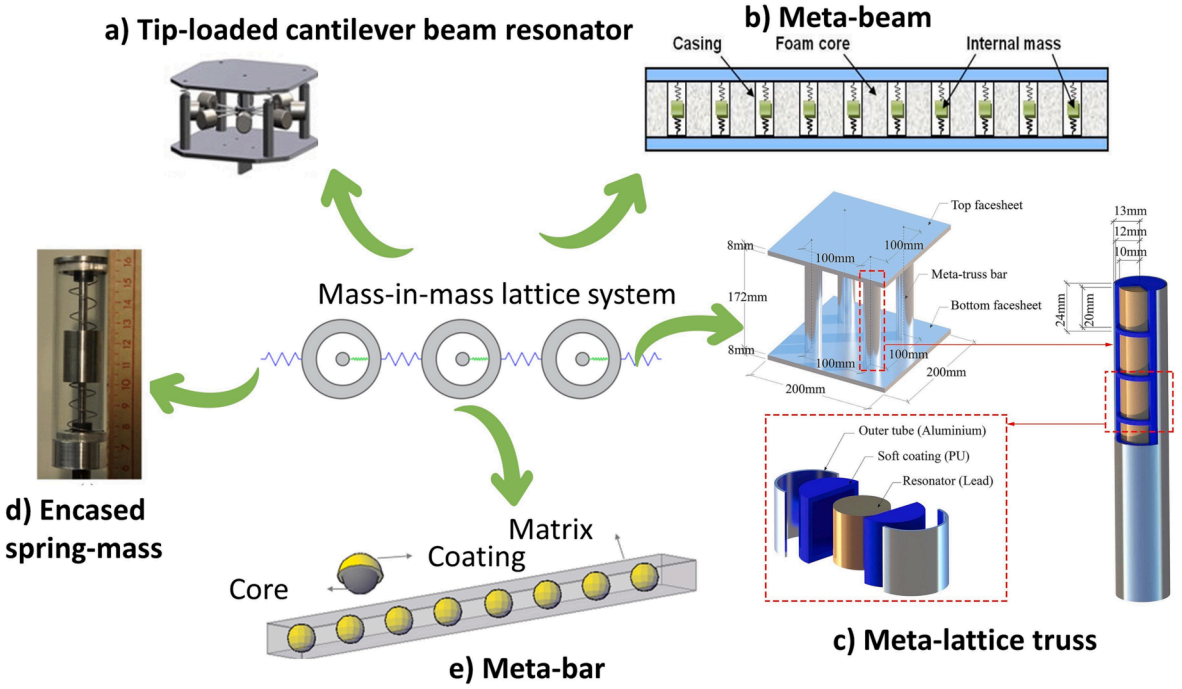

Fig. 7. Designs of locally resonant elements with axial translational resonance: a) Tip-loaded cantilever beam resonator. Copyright 2014, Elsevier [53]; b) Meta-beam. Copyright 2011, Elsevier [122]; c) Meta-lattice truss. Copyright 2022, Elsevier [58]; d) Encased spring-mass. Copyright 2014, Elsevier [53]; e) Meta-bar.

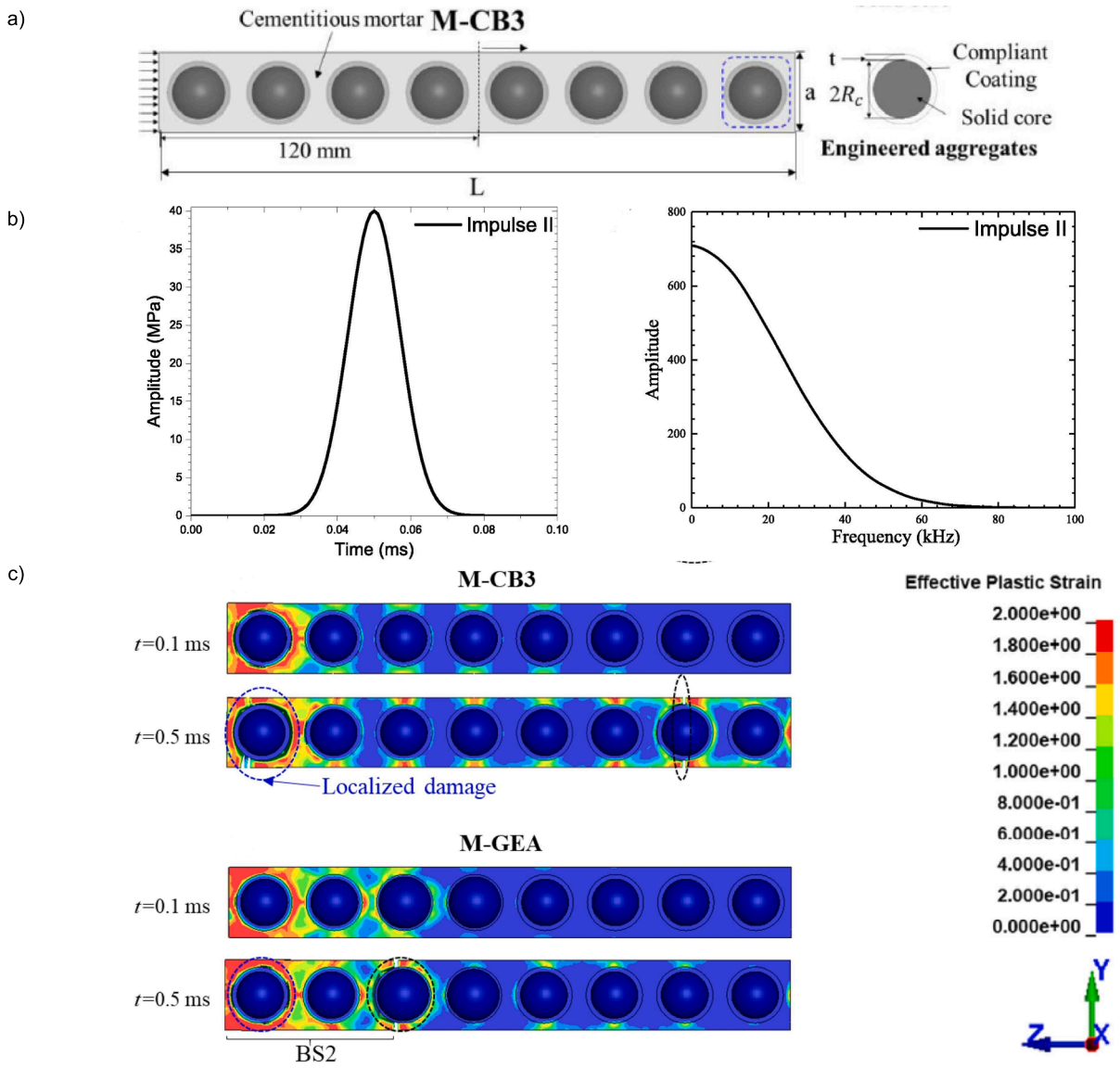

Fig. 8. Response of meta-concrete: a) Numerical simulation. Copyright 2021, Elsevier [102]; b) Load characteristics. Copyright 2021, Elsevier [102]; c) Distribution of plastic strain of the models. Copyright 2021, Elsevier [102].

fracture length of the meta-concrete bar was smaller than that of an ordinary concrete bar. A mesoscale model simulation of the second case [97] found that the stiffness difference between the matrix and coating resulted in stress concentration [97]. This difference in stiffness also reduced the spalling strength of the meta-concrete bar, leading to more severe fractures under tensile waves than concrete bars [97]. Consequently, adding a harder coating layer around the primary layer was desirable to increase the spalling strength of meta-concrete [124]. Different laboratory tests studied the wave attenuation effect of meta-concrete. Non-destructive dynamics tests were conducted on meta-concrete using ultra-sonic [125], sonic [126] and low-frequency-sonic waves [27,99]. Also, the wave attenuation effect under impact loading was assessed [96,127]. All these tests demonstrated the wave attenuation effect around the resonance frequency of the cores, confirming that locally resonant elements stored energy. Furthermore, the core order did not exhibit to affect the wave attenuation [99,125], and using more cores increased the stored energy capacity of meta-concrete [27,96,99,125,126]. Studies also quantified the static and dynamic meta-concrete material properties and proposed empirical relations for dynamic increase factor and energy dissipation curves for meta-concrete material [127].

Meta-concrete demonstrated the advantage of wave attenuation capacity, achieving a 77 % energy attenuation after interacting with three rows of cores [91]. The cores can be tuned to attenuate different loads with different frequencies. Significantly, the construction process of meta-concrete closely resembles that of regular concrete, making it more feasible for application [99,125]. Nevertheless, it should be noted that compared to regular concrete, meta-concrete often exhibits lower compressive and tensile strengths [124,128], and stress concentration is also more prone to develop around the cores [102].

5. Meta-structures with external resonators

In this paper, to be differentiated from meta-structures with internal resonators, meta-structures with external resonators are defined as an existing structure protected with an additional frontal panel (meta-truss, meta-sandwiches, and meta-beams) or surrounding shield (seismic metamaterials). This section reviews the applications of meta-structures with external resonators, which include meta-sandwiches, meta-trusses, meta-beams, and seismic metamaterials.

5.1. Meta-truss

Meta-truss exhibits an ultra-low frequency band gap attributed to the shear stiffness of its components, resulting in a widened band gap and enhanced wave filtering capacity. In the early days of research on locally resonant metamaterials, studies demonstrated that employing a fixed core or outer border could open an ultra-low frequency band gap [83,129]. Following the trend, Liu et al. [5] fixed steel bars around the matrix to activate its shear stiffness. This concept was adopted in meta-trusses with either single or dual-resonators. As illustrated in Fig. 9a, the meta-trusses design consisted of aluminium tubes filled with a layer of soft plastic, with heavy cylinders coated to form the locally resonate elements. Two face sheets were then used to laminate the tubes. Some researchers introduced an extra core and coating to produce dual-resonators (Fig. 9b).

Parametric analysis suggested that increasing the core mass, the coating matrix's shear stiffness and the matrix's shear stiffness could help widen band gaps [130]. A cuboid resonator showed to absorb energy more efficiently, while cylindrical resonators were easier to build [25]. Numerical studies compared the performance of meta-trusses with single [21,58] and dual-resonators [131] to traditional trusses [21,58,131] and hollow trusses [58,131]. Results exhibited that the cores of meta-trusses absorbed the majority of the energy, resulting in lower stress and deformation of the bottom face sheet compared to the non-meta counterparts. Besides the wave filtering capacity, the meta-truss created an asymmetric wave propagation effect if two resonators were used [30,31]. Vo et al. [26] conducted an experimental comparison involving a single-resonator meta-truss, a hollow truss, and a traditional truss. Under impact loading from a gas gun, the meta-truss absorbed 33 % of the total impact energy. Compared to the traditional truss, the meta-truss exhibited 19.1 % lower reaction force and 31.3 % less deformation, primarily attributed to the local vibration of the cores. In contrast, the hollow truss showed a 10.1 % reduction in reaction force and a 27.8 % reduction in deformation, primarily due to energy dissipation through the plastic deformation of truss bars. The meta-truss is considered a promising meta-structure with external resonators based on existing studies.

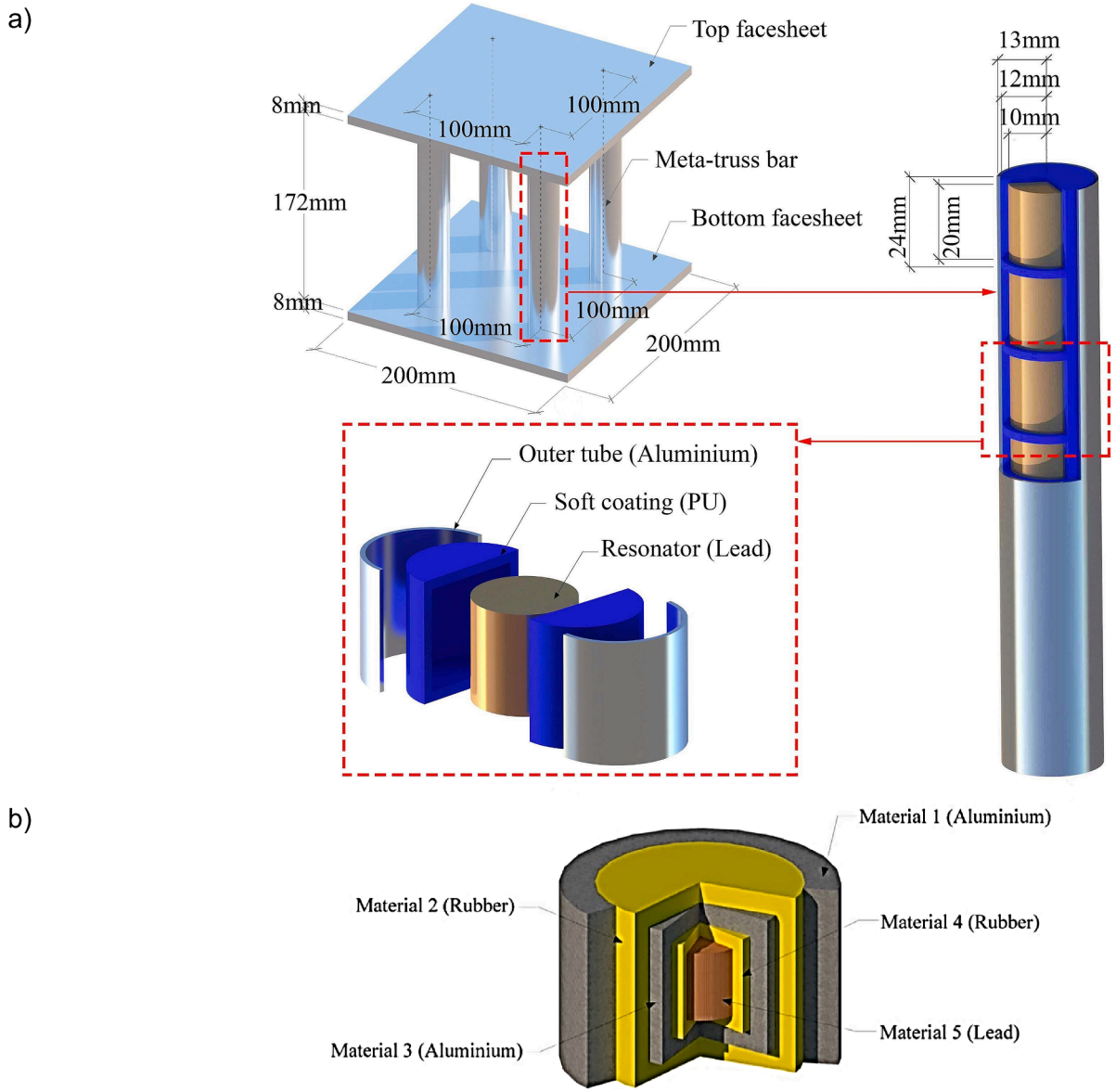

Fig. 9. a) Meta-panel, meta-truss, and a single resonator unit cell. Copyright 2022, Elsevier [58]; b) Dual-resonator unit cell. Copyright 2021, Elsevier [130].

5.2. Seismic metamaterials

Metamaterials offer the potential to mitigate seismic waves. Popular seismic meta-structures include seismic shields and periodic foundations. Seismic shields involve an array of elements embedded into the soil, producing a "shadow" that effectively filters seismic waves (Fig. 10a). This approach can be incorporated into existing structures to enhance their seismic resistance capacity [132]. On the other hand, for new structures, periodic foundations (Fig. 10b) can be designed to isolate seismic waves, which could mitigate ground motion in the vertical direction [133].

Existing studies have explored two types of seismic shields: periodic/photonic and locally resonant. For photonic shields, Brûlé et al. [135] conducted experimental investigations on a periodic array of piles embedded into the soil. These piles effectively attenuated Rayleigh waves in saturated and non-saturated soils [136]. Within locally resonant seismic shields, piles mounted on elastomeric bearings displayed the capacity to convert Rayleigh waves into bulk waves [137,138]. Forests exhibited a coupled mechanism involving longitudinal resonance and Rayleigh waves, which holds the potential to generate the desired filtering effect [139]. Helmholtz-type resonators successfully converted seismic energy into acoustic/heat energy [132]. An isochronous cycloidal pendulum showed reduced S-wave propagation by controlling the friction between the ball and the pendulum [140]. Meta-wedges exhibited the ability to reflect Rayleigh waves [141]. Meta-surfaces consist of an array of oscillators attached to the free surface of a half-space. These meta-surfaces demonstrated the ability to create band gaps centred around the natural frequency of the oscillators, thereby transforming Rayleigh waves into bulk waves. Moreover, some studies discovered approaches to enhance the performance of locally resonant seismic shields. Matryoshka-type seismic shields increased the band gaps [142,143], while ultra-heavy depleted uranium cores exhibited significant efficiency [93].

Numerical simulations demonstrated that the photonic periodic foundation reduced the inter-story drifts of a building subjected to seismic loads. However, the low horizontal stiffness of the foundation could also increase the absolute displacement of the structure [144]. Shaking table tests were conducted to assess the performance of periodic foundations [133,145], in which the peak acceleration exhibited a 50 % and 15 % reduction along the horizontal and vertical directions, respectively [145]. Furthermore, the local response of resonant periodic foundations was also investigated. Theoretical derivation showed that their performance outperformed regular structures [146]. 2-D and 3-D experimental tests demonstrated that the acceleration on the isolated structure was reduced, reflecting the ability to mitigate both the S and P waves [94,95]. Additionally, according to the Eurocode, researchers verified using metamaterials for constructing periodic foundations as load-bearing structures for seismic mitigation [147]. Recently, Zhou et al. [148] proposed using the basement slab of a building as a locally resonant element. They suggested isolators to facilitate the movement between the slab and the supporting beam. The system showed a numerical attenuation of 20 % of the structural responses.

5.3. Meta-sandwiches and meta-beams

Meta-sandwiches and meta-beams share the capacity to attenuate flexural waves and control the vibration of a structure. Sandwich structures comprise two external metal sheets and a core foam, extensively used as sacrificial structures to mitigate structural damage caused by impact and blast loadings [25]. Various sandwich panels designs can be found in the literature, such as cellular cores [149], kirigami folds [150], Bio-inspired [151], hollow trusses [152], and pyramidal lattice structures [153]. In 2011, Chen and Sun [122,154] conducted a theoretical analysis and found that fusing sandwich panels with locally resonant elements could mitigate the seismic response of structures subjected to flexural waves. The resulting hybrid structure was named "meta-sandwich" and composed of two external face sheets laminating a foam surrounding spring-mass systems, as illustrated in Fig. 11a. Sharma and Sun [155] built a standard sandwich and meta-sandwich panel. When subjected to the same impact loading, the flexural strain of the meta-beam was significantly lower than the measured one in the reference beams. Therefore, meta-sandwich panels could effectively enhance the strength of the system.

Researchers have mainly analysed meta-beams made with locally resonant elements attached to beams, as illustrated in Fig. 11b. Yu et al. [156,157] investigated the concept of constructing a circular beam encircled by rubber rings that connected the beam with copper rings (Fig. 11c). Results revealed the formation of flexural band gaps, which proved optimal for vibration control. Regarding meta-beam design, studies suggested that attaching resonators with smaller masses is more efficient than fewer resonators with larger masses [158]. Moreover, they noted that meta-beams could generate ultra-low frequency band gaps when built with flexible supports [159] or applied to a Winkler foundation [160].

6. Approaches to enhance the band gap

Locally resonant metamaterials effectively absorb the imposed energy within the band gaps. Large band gaps increase the energy absorption capacity of a metamaterial. Much effort has been made to develop new methods for enhancing the band gaps of metamaterials [20,105,161,162]. Research demonstrated that increasing the core mass, using a lighter matrix, and decreasing the stiffness of the coating could all help to enlarge the band gap [104]. However, for civil engineering applications, the available space limits the core mass, while reducing the coating stiffness would also decrease the structural strength. To overcome these limitations, different approaches have been introduced, including nonlinearities [161,163], inertial amplification [164–168], and meta-damping [70,101,109,169–171]. This section reviews these approaches.

6.1. Multiple resonances

Band gaps emerge around the resonance frequency of locally resonant elements. Thus, adding multiple resonators to generate band gaps

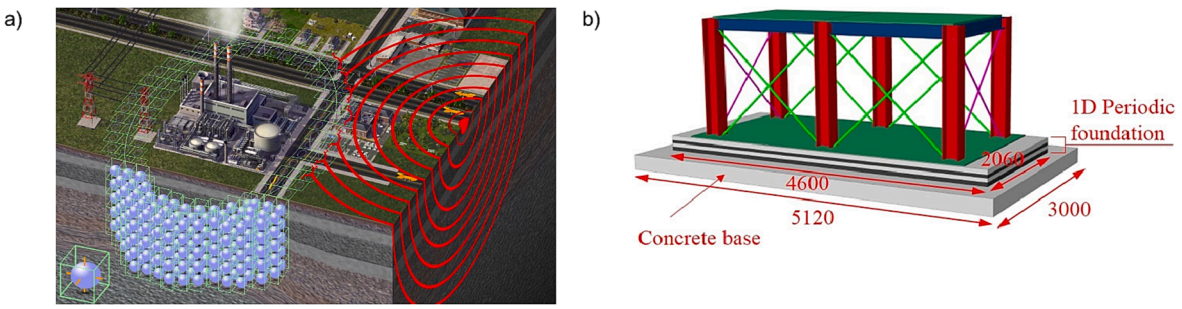

Fig. 10. a) Schematization of a seismic shield. CC BY 4.0 [134]; b) Schematization of a periodic foundation. CC BY 4.0 [133].

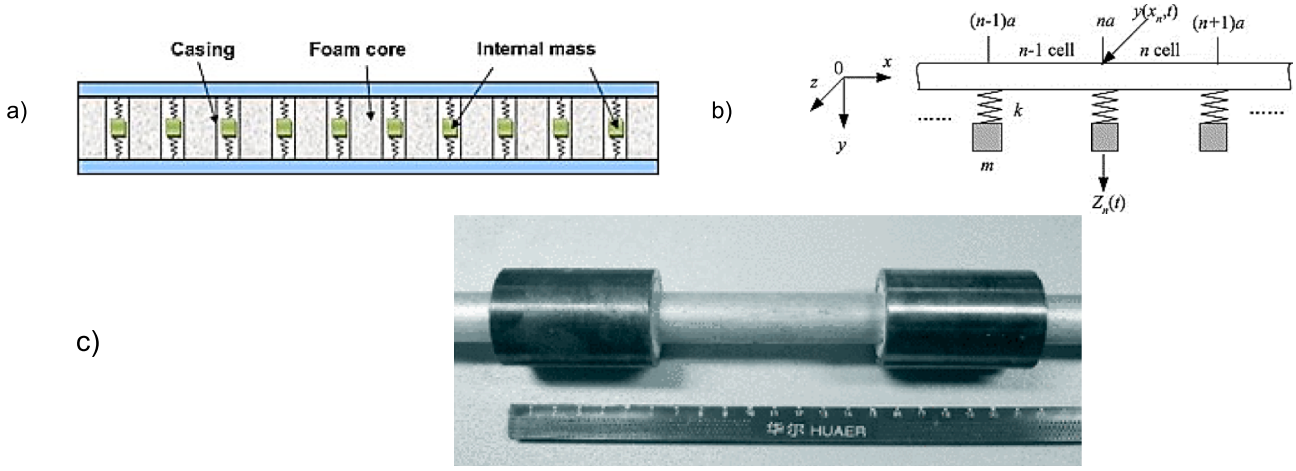

Fig. 11. a) Meta-sandwich structure. Copyright 2011, Elsevier [122]; b) Simplified model of a meta-beam. Copyright 2007, Elsevier [158]; (c) Meta-beam design. Copyright 2006, American Physics Society [156].

at different frequencies is a simple and intuitive method to widen the band gap. There are two main streams of multiple resonators: (1) similar to the mass-in-mass lattice system of Fig. 2a, every unit-cell presents a different matrix, core and coating (graded systems) [172]; (2) by introducing dual-resonators. As illustrated in Fig. 12, dual-resonators introduce an extra-coated core inside or outside the main core of a mass-in-mass lattice system. Both methods generate new band gaps that mitigate waves at the resonance frequencies of the resonators [105,173]. It is worth noting that equations in Section 3 can be used to calculate the band gaps of the first stream. Huang & Sun [173] derived an expression for the band gap of dual-resonators.

Theoretical studies optimised systems with multiple resonators. Banerjee et al. [172] analysed the effects of considering each unit cell with different core masses, resonator stiffnesses, matrix masses, and matrix stiffnesses. They concluded that grading the stiffness would have a more substantial effect than grading the mass. Moreover, a meta-beam with multiple arrays exhibited a wider band gap. Nevertheless, the attenuation effect was less significant than using one array of resonators [174]. Furthermore, Tan et al. [51] compared the performance of a system with dual-resonators and two different coated cores. The dual-resonator system required fewer unit cells to perform similarly to a system with two single resonators.

The acoustic field initiated practical applications of multiple resonances when researchers detected an ultra-wide band gap in a system of

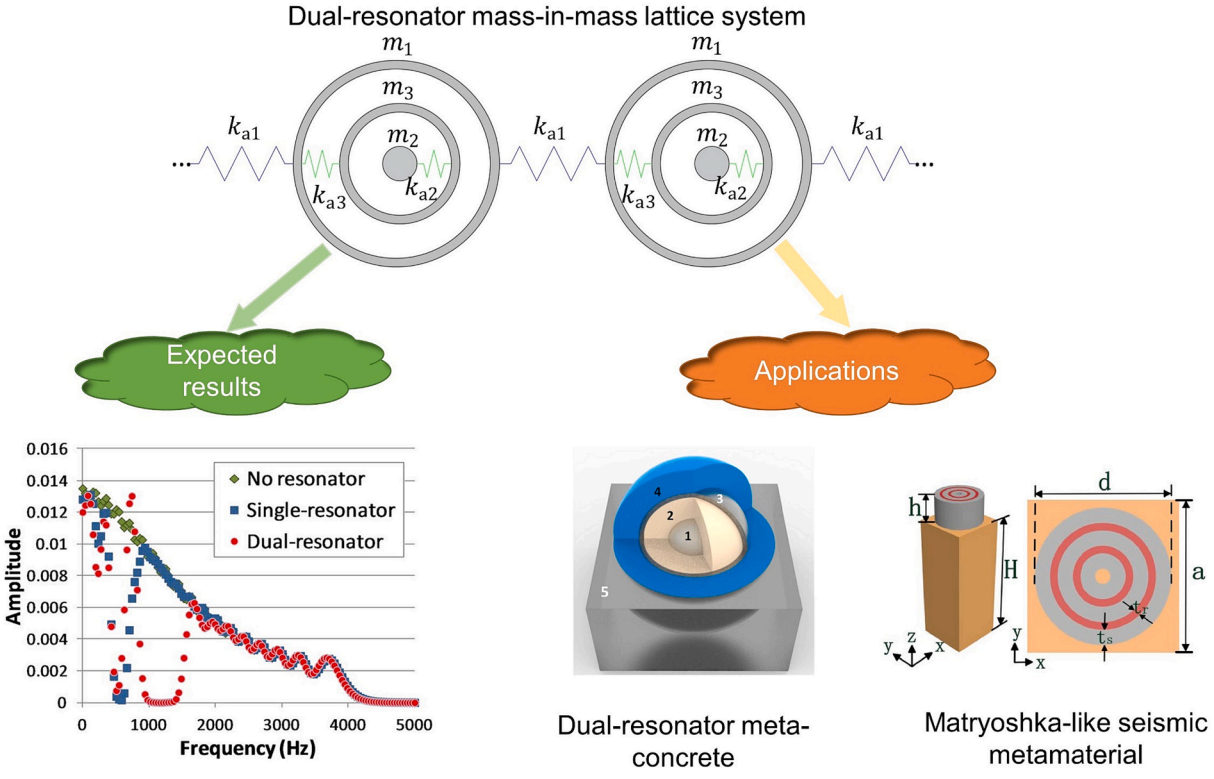

Fig. 12. Illustration of a Dual-resonator response scenario encompassing expected results and applications. The expected results offer a comparative analysis between a single resonator and a dual-resonator configuration. Copyright 2012, AIP Publishing [105]. The applications showcase specific instances, namely, the integration of the dual-resonator within meta-concrete. Copyright 2019, Elsevier [171]; and the concept of a Matryoshka-like Seismic Metamaterial. Copyright 2020, Elsevier [142].$\boldsymbol{m}_3$ = Mass of the second resonator; $\boldsymbol{k}_{a3}$= Axial stiffness of the second coating.

stacked membranes with different natural frequencies [175–177]. In civil engineering, researchers utilized graded systems to enhance the energy absorption performance of meta-concrete by creating new band gaps [102]. Researchers also identified these new band gaps in chains of resonators subjected to impact loads, noting that they increased the attenuation of the systems [53,106]. Matryoshka-like seismic meta-materials [142] and meta-concrete structures [91,171] (Fig. 12) demonstrated to have a notable band gap widening performance.

6.2. Nonlinearities

Material nonlinearities [161,163] and leaks in the velocity function [178–180] exhibited to improve the energy dissipation capacity of metamaterials. Mass-in-mass spring mass lattice systems with nonlinear softening and hardening effects have been demonstrated to expand the band gap [163]. Nonlinearities found an application in developing meta-surfaces constructed with an array of Duffing oscillators. Studies on nonlinear meta-surfaces applied to layered and non-layered soils revealed that the hardening effect neglected the emergence of a band gap. In contrast, the softening effect could shift the band gap to lower frequencies [181,182]. Additionally, it was observed that the amplitude of the load could increase the effect of the nonlinearities [181,182], and these nonlinearities also influenced the dispersion of third harmonics [181]. Specifically, the hardening effect could result in a band gap dependent solely on the parameters of the linear meta-surface. The dispersion analysis of third harmonic waves showed that the fundamental band gap corresponds to a valley interval for the third harmonics. Another significant application involves nonlinear acoustic meta-beams with attached Duffing oscillators, where the meta-beams with nonlinear softening behaviour exhibited a flexural band gap starting from 0 Hz, which was wider than when linear springs were used [183]. Granular chains composed of axial translational resonators exhibited a band gap that changes with the applied pre-compression force [184].

Pounding between the core and the matrix improved the energy dissipation performance of metamaterials [178–180]. Banerjee et al. [178] numerically studied a stereo-mechanical system considering multiple poundings per cycle and noted four responses: multiperiodic response, chaotic response, sticking response, and response without pounding. The multiperiodic response greatly enhanced the band gap, while the chaotic response enhanced the response in specific band gaps. The sticking and without-pounding responses appeared to have negligible influence on the response of the system. Later, a parametric study found that the multiperiodic response produced an out-of-phase motion even if its non-pounding equivalent model was in an in-phase motion [179]. Furthermore, the pounding systems required a smaller mass to generate the same band gap as the non-pounding systems [179]. A chain with five pounding units extended previous studies [180]. Adding new unit cells significantly widened the band gap and the attenuation effect. Moreover, almost all impacts occurred during the steady vibration phase [180].

6.3. Meta-damping

Most studies of locally resonant metamaterials focused on the transient state response and neglected material damping. Nevertheless, damping is an intrinsic characteristic of the materials, and it is essential to clarify its effect on the band gap to accurately understand the response of the meta-structure in the steady state. Investigations have noted that the combination of viscous damping and locally resonant elements increased the system's damping ratio, a phenomenon called "meta-damping" [53,169]. Meta-damping introduced a new energy absorption mechanism that operates simultaneously with the locally resonant elements. Initially, meta-damping received criticism for narrowing the band gap and reducing the wave attenuation produced by the locally resonant elements [70,169]. Nonetheless, meta-damping exhibited to dissipate the stored energy in the resonating element and thus reduced the reflected energy [169]. Several researchers proposed the construction of more effective wave attenuation materials by integrating locally resonant elements with meta-damping [109]. Moreover, considering the damping of the coating layer proved more advantageous than accounting for the damping of the matrix, as the high core velocities can significantly enhance wave attenuation [109]. Furthermore, friction between the core and the matrix induced viscous meta-damping, enhancing the wave attenuation effect for high frequencies [185].

Barnhart et al. [171] investigated meta-damping on an epoxy meta-rod made of dual-resonators (Fig. 13a). They noted that the system expanded the band gap width, which numerical simulation proved to be caused by the meta-damping (Fig. 13b). Similar theoretical studies employed Maxwell-type oscillators [186] and Kelvin-Voight spring dampers [170]. Similar phenomena emerged in systems with cubic Duffing nonlinearities [187] and meta-surfaces with inerters [188], where two peaks can also combine by increasing the damping. Furthermore, theoretical analyses of meta-damping in meta-sandwich structures concluded that damping dramatically increased around the local resonance frequency, which helped to dissipate the kinetic energy stored in the resonator [121]. Moreover, some researchers discovered that meta-damping might lead to 96 % of the damping ratio of a meta-concrete bar [101]. Therefore, proper consideration of meta-damping could be an effective and efficient measure to improve the energy dissipation capacity of metamaterials.

6.4. Other mechanisms

Increasing the inertial force has also improved the performance of metamaterials. A typical and practical method for increasing the inertial force is to attach a rigid lever and a mass to the principal system (Fig. 14a). The lever amplifies the movement of the attached mass, increasing the total response of the system. In periodic metamaterials, inertial amplification shifted the band gap to lower frequencies [164,167]. On the other hand, locally resonant metamaterials with inertial amplification displayed a new band gap linked to the inertial amplification [165]. The band gaps could be fused with the locally resonant band gap [165]. Moreover, a comparison between the performance of meta-beams with multiple locally resonant elements and inertial amplifications revealed that multiple-local resonances (red dashed line in Fig. 14b) produced more prominent attenuation effects [166]. However, the band gap is much narrower than that produced by the inertial amplification effect (Blue line in Fig. 14b).

Another method to increase the inertial force is using inerters. The inerter is the mechanical analogue of a capacitor, and consequently, it ideally produces a force proportional to the difference in acceleration between ports [189]. The primary inerter designs were rack-and-pinion and ballscrew inerter [190], which transformed the differential movement between terminals into rotational motion. In its early years, inerters showed a remarkable improvement in the mechanical grip in racing cars [191], leading to rapid adoption in various applications, including building suspensions [192] and passive structural vibration control [193]. Researchers also attempted to use inerters to enhance the response of locally resonant elastic metamaterials. They were particularly interested in the apparent increase in mass [193] and the decrease in the natural frequencies of the system produced by the inerters [194,195].

Kulkarni and Manimala [168] analysed potential locations for the inerter within the mass-in-mass lattice system. They explored four configurations: (a) Inerter in series with the coating spring, (b) Inerter in series with the matrix spring, (c) Inerter in parallel with the coating spring, and (d) Inerter in parallel with the matrix spring. The analysis revealed that the band gap of configuration (a) shifted to higher frequencies. On the contrary, the band gap of configuration (c) shifted to lower frequencies. Configurations (b) and (d) showed the emergence of new band gaps at higher and ultra-low frequencies, respectively. Ba'ba'a

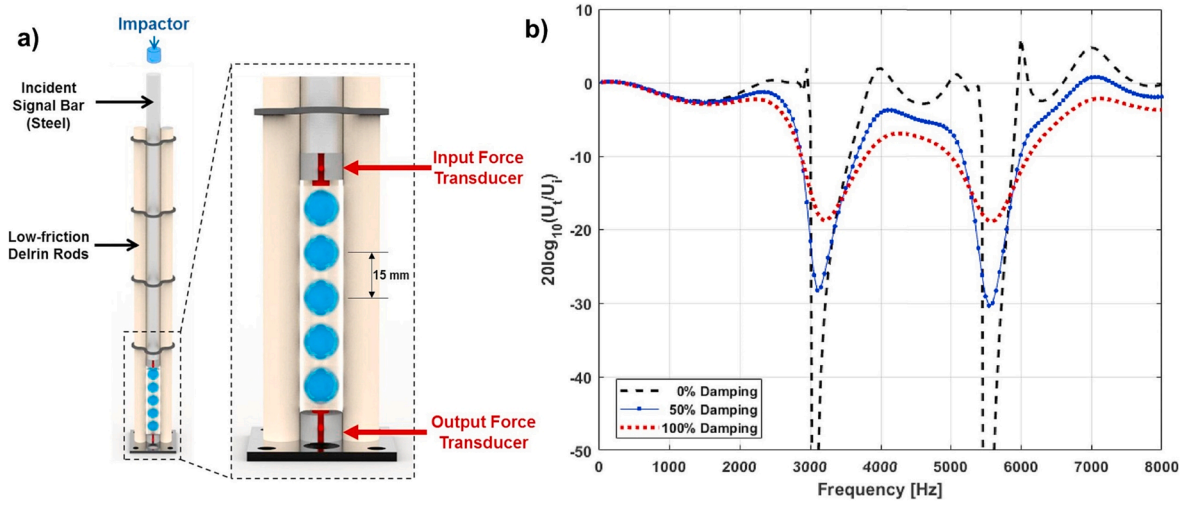

Fig. 13. A) Experimental setup employed for the investigation of the meta-damping phenomenon. Copyright 2019, Elsevier [171]; b) Numerical simulation demonstrating an ultra-wide band gap generation through meta-damping. Copyright 2019, Elsevier [171].

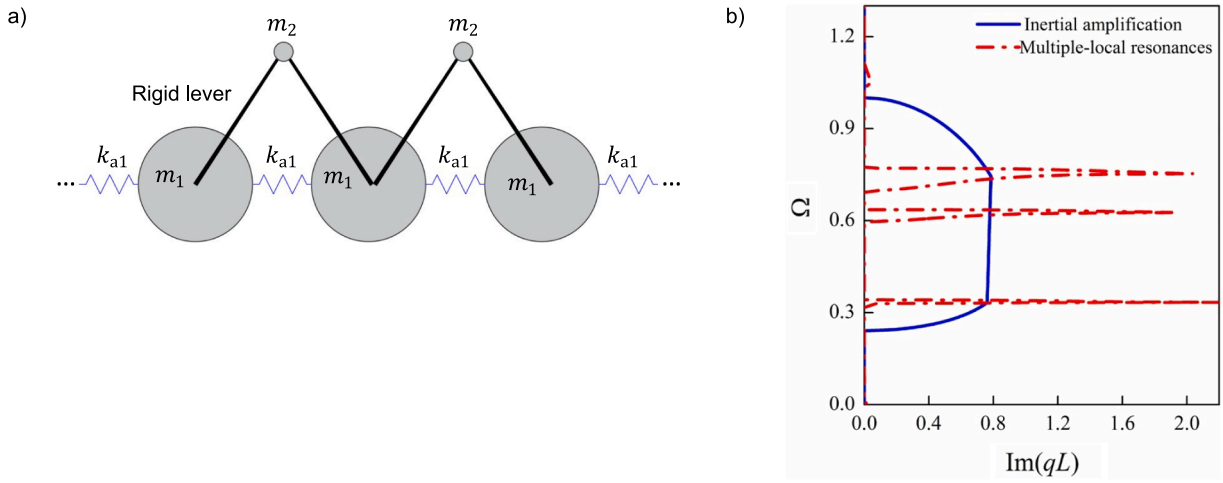

Fig. 14. A) Schematic depiction of a lattice system featuring inertial amplification; b) comparative illustration of the dispersion relation between a meta-beam with multiple local resonances and a meta-beam with inertial amplifications. Copyright 2018, Elsevier [166].

et al. [196] investigated a configuration with the inerter connected in parallel with the coating and matrix spring, determining the conditions for combining the band gap of the locally resonant element with the band gap of the matrix inerter.

Applying inerters in seismic metamaterials has facilitated the design of more compact vibrating barriers [197]. Locally resonant periodic foundations with a tuned inerter damper located at the ground floor demonstrated a decrease in the normalised maximum peak response [198]. Moreover, the band gap was lowered to 2–12 Hz [199]. However, increasing inertial forces could create extra seismic demands on the foundations, requiring a more robust design [193]. Numerical simulations demonstrated that a meta-surface with inerter-based vibration absorbers (IDVAs) created two band gaps, converting surface waves to bulk waves. The band gaps, attributed to the local resonator and IDVAs, could be adjusted using the inerter ratio and stiffness. Higher stiffness ratios widened both band gaps, while increasing the inerter ratio lowered the resonator band gap frequency and widened the IDVA band gap with a higher central frequency [188]. Meta-beams/plates with inerter-based dynamic vibration absorbers outperformed the design with standard dynamic vibration absorbers [200,201]. Moreover, meta-beams with inerters connected to the ground exhibited a higher damping order of magnitude than non-inerted systems [202].

Combining the Bragg scattering effect with resonances is an intriguing mechanism for enhancing the band gap. The combined effects were studied in meta-rods [72], meta-beams [203] and phononic crystal rods [204]. Studies demonstrated that the band gaps almost fully merged when the natural frequency of the locally resonant element equalled the terminal frequency of the Bragg scattering band gap. However, if the natural frequency fell between the initial and terminal frequency of the Bragg scattering band gaps, it would broaden the locally resonant band gap at the expense of the Bragg scattering band gap [204]. Moreover, it was discussed that a band gap twice as wide as the Bragg scattering gap could be achieved by utilizing the matrix of a metamaterial as a Bragg scatterer [205]. On the other hand, Matlack et al. [206] argued that it is feasible to tune the band gap limits by modifying the mode shape of a structure. A polycarbonate lattice with embedded steel cubes as coated cores were built to prove this concept. The natural frequencies were altered by removing beams, resulting in band gaps with lower limits.

7. Conclusions and future outlook

7.1. Concluding remarks

This paper presents a comprehensive review of the history and the latest progress in applying locally resonant metamaterials in civil engineering. The history of metamaterials is initially introduced to explain their origins and branches. A classification is proposed to provide context for applying metamaterials in civil engineering. Then, various resonant mechanisms and their effects on effective linear elastic properties are described. Theoretical and numerical simulation methods for determining the band gap are reviewed, and their application to different designs is contrasted and discussed. The review includes an examination of existing applications of meta-structures with internal and external resonators. Notably, meta-concrete, a primary type of metamaterial with internal resonators, is highlighted. The energy absorption mechanism of locally resonant elements, which attenuate stress waves and reflects the energy associated with the band gap, is explained. For metamaterials with internal and external resonators, prominent designs with potential for civil engineering applications are summarised, highlighting their advantages and detailed performances.

7.2. Future outlook

Existing studies on metamaterials primarily exist within theoretical realms, often lacking direct engineering applications. Current investigations rely on simplified models [53] and small-scale numerical simulations [81], such as meta-bars [96], meta-trusses [26], and meta-mortar blocks [107]. However, significant gaps exist without comprehensive validations for intricate engineering-like structures. Moreover, diverse methods for enhancing band gaps are explored in the literature. However, critical concepts such as friction and pounding within the core-matrix interface remain unverified. The feasibility of these concepts in engineering applications also remains largely unverified.

Many civil engineering applications require meta-structures with low-frequency band gaps. This is crucial for vibration control, earthquake protection, or impact reduction at low speeds. However, a challenge arises due to the small size of resonators, which makes it challenging to design resonators that work at these low frequencies while fitting within materials or structures. Several potential solutions to this problem exist. One option is to increase the size and weight of the resonator core, which could lower its natural frequency. Another approach involves reducing the stiffness of the coating material or adjusting its shear stiffness, potentially facilitating the creation of an ultra-low frequency band gap. These concepts require further research to assess their feasibility. Another avenue is to employ special auxetic coatings, which could enhance material rigidity by altering its properties. However, this approach necessitates more in-depth analysis and testing to ensure its intended functionality.

CRediT authorship contribution statement

Nicolás Contreras: Investigation, Conceptualization, Visualization, Writing – original draft. **Xihong Zhang:** Resources, Writing – review & editing, Supervision, Funding acquisition, Project administration. **Hong Hao:** Resources, Supervision, Writing – review & editing. **Francisco Hernández:** Writing – review & editing.

Declaration of Competing Interest

The authors declare that they have no known competing financial interests or personal relationships that could have appeared to influence the work reported in this paper.

Data availability

No data was used for the research described in the article.

Acknowledgement

The authors would like to acknowledge the financial support from Australian Research Council [DE210100986].

References

[1] Pendry JB. Negative refraction makes a perfect lens. Phys Rev Lett 2000;85(18):3966–9.
[2] Cai W, Shalaev V. Introduction. In: Cai W, Shalaev V, editors. Optical Metamaterials: Fundamentals and Applications. Springer, New York: New York, NY; 2010. p. 1–10.
[3] Sigalas MM, Economou EN. Elastic and acoustic wave band structure. J Sound Vib 1992;158(2):377–82.
[4] Simovski CR. Material parameters of metamaterials (a Review). Opt Spectrosc 2009;107(5):726–53.
[5] Liu Y, Shen X, Su X, Sun CT. Elastic Metamaterials With Low-Frequency Passbands Based on Lattice System With On-Site Potential. J Vib Acoust 2016;138(2):021011.
[6] Askari M, Hutchins DA, Thomas PJ, Astolfi L, Watson RL, Abdi M, et al. Additive manufacturing of metamaterials: A review. Addit Manuf 2020;36:101562.
[7] Hussein MI, Leamy MJ, Ruzzene M. Dynamics of Phononic Materials and Structures: Historical Origins, Recent Progress, and Future Outlook. Appl Mech Rev 2014;66(4).
[8] Liu Z, Zhang X, Mao Y, Zhu YY, Yang Z, Chan CT, et al. Locally resonant sonic materials. Science 2000;289(5485):1734–6.
[9] Hirsekorn M, Delsanto PP, Leung AC, Matic P. Elastic wave propagation in locally resonant sonic material: Comparison between local interaction simulation approach and modal analysis. J Appl Phys 2006;99(12). pp. 124912–124912-124918.
[10] Sheng P, Zhang XX, Liu Z, Chan CT. Locally resonant sonic materials. Phys B Condens Matter 2003;338(1–4):201–5.
[11] Mei J, Liu Z, Wen W, Sheng P. Effective mass density of fluid-solid composites. Phys Rev Lett 2006;96(2):024301.
[12] Li J, Chan CT. Double-negative acoustic metamaterial. Phys Rev E Stat Nonlin Soft Matter Phys 2004;70(5 Pt 2):055602.
[13] Chan CT, Li J, Fung KH. On extending the concept of double negativity to acoustic waves. J Zhejiang Univ-Sci A 2006;7(1):24–8.
[14] Wu Y, Lai Y, Zhang Z-Q. Effective medium theory for elastic metamaterials in two dimensions. Phys Rev B 2007;76(20):205313.
[15] Liu Z, Chan CT, Sheng P. Analytic model of phononic crystals with local resonances. Phys Rev B 2005;71(1). 014103.014101-014103.014108.
[16] Banerjee A, Das R, Calius EP. Waves in Structured Mediums or Metamaterials: A Review. Arch Comput Meth Eng 2018;26(4):1029–58.
[17] Liu X, Hu G. Elastic Metamaterials Making Use of Chirality: A Review. Strojniški vestnik - J Mech Eng 2016;62(7–8):403–18.
[18] Bilal OR, Hussein MI. Trampoline metamaterial: Local resonance enhancement by springboards. Appl Phys Lett 2013;103(11):111901.
[19] Srivastava A. Elastic metamaterials and dynamic homogenization: a review. Int J Smart Nano Mater 2015;6(1):41–60.
[20] Liu Y, Su X, Sun CT. Broadband elastic metamaterial with single negativity by mimicking lattice systems. J Mech Phys Solids 2015;74:158–74.
[21] Li B, Liu Y, Tan K-T. A novel meta-lattice sandwich structure for dynamic load mitigation. J Sandw Struct Mater 2017;21(6):1880–905.
[22] Vo NH, Pham TM, Hao H, Bi K, Chen W. A reinvestigation of the spring-mass model for metamaterial bandgap prediction. Int J Mech Sci 2022;221:107219.
[23] Huang HH, Sun CT, Huang GL. On the negative effective mass density in acoustic metamaterials. Int J Eng Sci 2009;47(4):610–7.
[24] Bo Z, Li Z. New Analytical Model for Composite Materials Containing Local Resonance Units. J Eng Mech 2011;137(1):1–7.
[25] Vo NH, Pham TM, Hao H, Bi K, Chen W, Ha NS. Blast resistant enhancement of meta-panels using multiple types of resonators. Int J Mech Sci 2022;215:106965.
[26] Vo NH, Pham TM, Hao H, Bi K, Chen W. Experimental and numerical validation of impact mitigation capability of meta-panels. Int J Mech Sci 2022;231:107591.
[27] Briccola D, Pandolfi A. Analysis on the Dynamic Wave Attenuation Properties of Metaconcrete Considering a Quasi-Random Arrangement of Inclusions. Front Mater 2021;7.
[28] Lai Y, Wu Y, Sheng P, Zhang ZQ. Hybrid elastic solids. Nat Mater 2011;10(8):620–4.
[29] Huang HH, Sun CT. Locally resonant acoustic metamaterials with 2D anisotropic effective mass density. Phil Mag 2011;91(6):981–96.
[30] Li B, Tan KT. Asymmetric wave transmission in a diatomic acoustic/elastic metamaterial. J Appl Phys 2016;120(7):075103.
[31] Li B, Alamri S, Tan KT. A diatomic elastic metamaterial for tunable asymmetric wave transmission in multiple frequency bands. Sci Rep 2017;7(1):6226.
[32] Barber DJ, Freestone IC. An Investigation of the Origin of the Colour of the Lycurgus Cup by Analytical Transmission Electron Microscopy. Archaeometry 1990;32(1):33–45.

[33] Bose JC. On the Rotation of Plane of Polarisation of Electric Waves by a Twisted Structure. Proc Royal Soc Lond 1898;63:146–52.
[34] Rayleigh LXVII. On the maintenance of vibrations by forces of double frequency, and on the propagation of waves through a medium endowed with a periodic structure. Lond, Edinburgh, Dublin Philos Magaz J Sci 2009;24(147):145–59.
[35] Yu X, Zhou J, Liang H, Jiang Z, Wu L. Mechanical metamaterials associated with stiffness, rigidity and compressibility: A brief review. Prog Mater Sci 2018;94:114–73.
[36] Li W, Meng F, Chen Y, Yf Li, Huang X. Topology Optimization of Photonic and Phononic Crystals and Metamaterials: A Review. Adv Theory Simul 2019;2(7). 1900017-n/a.
[37] Vivek A, Shambavi K, Alex ZC. A review: metamaterial sensors for material characterization. Sens Rev 2019;39(3):417–32.
[38] Muhammad LCW. From Photonic Crystals to Seismic Metamaterials: A Review via Phononic Crystals and Acoustic Metamaterials. Arch Comput Meth Eng 2021;29(2):1137–98.
[39] Kumar R, Kumar M, Chohan JS, Kumar S. Overview on metamaterial: History, types and applications. Mater Today: Proc 2022;56:3016–24.
[40] Ji G, Huber J. Recent progress in acoustic metamaterials and active piezoelectric acoustic metamaterials - A review. Applied. Mater Today 2022;26:101260.
[41] Xiao S, Wang T, Liu T, Zhou C, Jiang X, Zhang J. Active metamaterials and metadevices: a review. J Phys D Appl Phys 2020;53(50):503002.
[42] Veselago VG. The electrodynamics of substances with simultaneously negative values of ϵ And μ. Soviet Phys Uspekhi 1968;10(4):509–14.
[43] Yablonovitch E. Inhibited spontaneous emission in solid-state physics and electronics. Phys Rev Lett 1987;58(20):2059–62.
[44] Martínez-Sala R, Sancho J, Sánchez JV, Gómez V, Llinares J, Meseguer F. Sound attenuation by sculpture. Nature 1995;378(6554):241.
[45] Smith DR, Padilla WJ, Vier DC, Nemat-Nasser SC, Schultz S. Composite medium with simultaneously negative permeability and permittivity. Phys Rev Lett 2000;84(18):4184–7.
[46] Shelby RA, Smith DR, Schultz S. Experimental verification of a negative index of refraction. Science 2001;292(5514):77–9.
[47] Dalela S, Balaji PS, Jena DP. A review on application of mechanical metamaterials for vibration control. Mech Adv Mater Struct 2021;29(22):3237–62.
[48] Zadpoor AA. Mechanical meta-materials. Mater Horiz 2016;3(5):371–81.
[49] Wu W, Hu W, Qian G, Liao H, Xu X, Berto F. Mechanical design and multifunctional applications of chiral mechanical metamaterials: A review. Mater Des 2019;180:107950.
[50] Ren X, Das R, Tran P, Ngo TD, Xie YM. Auxetic metamaterials and structures: a review. Smart Mater Struct 2018;27(2):23001.
[51] Tan KT, Huang HH, Sun CT. Blast-wave impact mitigation using negative effective mass density concept of elastic metamaterials. Int J Impact Eng 2014;64:20–9.
[52] Bauer J, Schroer A, Schwaiger R, Kraft O. Approaching theoretical strength in glassy carbon nanolattices. Nat Mater 2016;15(4):438–43.
[53] Manimala JM, Huang HH, Sun CT, Snyder R, Bland S. Dynamic load mitigation using negative effective mass structures. Eng Struct 2014;80:458–68.
[54] Buckmann T, Thiel M, Kadic M, Schittny R, Wegener M. An elasto-mechanical unfeelability cloak made of pentamode metamaterials. Nat Commun 2014;5(1):4130.
[55] Yang L, Harrysson O, West H, Cormier D. Mechanical properties of 3D re-entrant honeycomb auxetic structures realized via additive manufacturing. Int J Solids Struct 2015;69–70:475–90.
[56] Peretokin AV, Stepikhova MV, Novikov AV, Dyakov SA, Zinovieva AF, Smagina ZV, et al. Photonic crystal band structure in luminescence response of samples with Ge/Si quantum dots grown on pit-patterned SOI substrates. Photonics Nanostruct Fundam Appl 2023;53:101093.
[57] Castro PJ, Barroso JJ, Leite Neto JP, Tomaz A, Hasar UC. Experimental Study of Transmission and Reflection Characteristics of a Gradient Array of Metamaterial Split-Ring Resonators. J Microw, Optoelectron Electromagnet Appl 2016;15(4):380–9.
[58] Vo NH, Pham TM, Hao H, Bi K, Chen W. Impact load mitigation of meta-panels with single local resonator. Eng Struct 2022;265:114528.
[59] Abbad A, Atalla N, Ouisse M, Doutres O. Numerical and experimental investigations on the acoustic performances of membraned Helmholtz resonators embedded in a porous matrix. J Sound Vib 2019;459:114873.
[60] Goto AM, Nóbrega ED, Pereira FN, Dos Santos JMC. Numerical and experimental investigation of phononic crystals via wave-based higher-order rod models. Int J Mech Sci 2020;181:105776.
[61] Wang G, Wen X, Wen J, Shao L, Liu Y. Two-dimensional locally resonant phononic crystals with binary structures. Phys Rev Lett 2004;93(15):154302.
[62] Gang W, Yao-Zong L, Ji-Hong W, Dian-Long Y. Formation mechanism of the low-frequency locally resonant band gap in the two-dimensional ternary phononic crystals. Chin Phys 2006;15(2):407–11.
[63] Berryman JG. Long-wavelength propagation in composite elastic media II. Ellipsoidal inclusions. J Acoust Soc Am 1980;68(6):1820–31.
[64] Liu XN, Hu GK, Sun CT, Huang GL. Wave propagation characterization and design of two-dimensional elastic chiral metacomposite. J Sound Vib 2011;330(11):2536–53.
[65] Liu XN, Hu GK, Huang GL, Sun CT. An elastic metamaterial with simultaneously negative mass density and bulk modulus. Appl Phys Lett 2011;98(25):251907.
[66] Huang HH, Sun CT. Theoretical investigation of the behavior of an acoustic metamaterial with extreme Young's modulus. J Mech Phys Solids 2011;59(10):2070–81.
[67] Zhou X, Liu X, Hu G. Elastic metamaterials with local resonances: an overview. Theor Appl Mech Lett 2012;2(4):041001.
[68] Mitchell SJ, Pandolfi A, Ortiz M. Metaconcrete: designed aggregates to enhance dynamic performance. J Mech Phys Solids 2014;65:69–81.
[69] Ma G, Fu C, Wang G, Del Hougne P, Christensen J, Lai Y, et al. Polarization bandgaps and fluid-like elasticity in fully solid elastic metamaterials. Nat Commun 2016;7(1):13536.
[70] Liu Y, Yi J, Li Z, Su X, Li W, Negahban M. Dissipative elastic metamaterial with a low-frequency passband. AIP Adv 2017;7(6):065215.
[71] Pai PF. Metamaterial-based Broadband Elastic Wave Absorber. J Intell Mater Syst Struct 2010;21(5):517–28.
[72] Xiao Y, Wen J, Wen X. Longitudinal wave band gaps in metamaterial-based elastic rods containing multi-degree-of-freedom resonators. New J Phys 2012;14(3):33042.
[73] Wang G, Wen J, Liu Y, Wen X. Lumped-mass method for the study of band structure in two-dimensional phononic crystals. Phys Rev B 2004;69(18):184302.
[74] Hirsekorn M, Delsanto PP, Batra NK, Matic P. Modelling and simulation of acoustic wave propagation in locally resonant sonic materials. Ultrasonics 2004;42(1–9):231–5.
[75] Hirsekorn M. Small-size sonic crystals with strong attenuation bands in the audible frequency range. Appl Phys Lett 2004;84(17):3364–6.
[76] Gang W, Li-Hui S, Yao-Zong L, Ji-Hong W. Accurate evaluation of lowest band gaps in ternary locally resonant phononic crystals. Chin Phys 2006;15(8):1843–8.
[77] Wang G, Wen X, Wen J, Liu Y. Quasi-One-Dimensional Periodic Structure with Locally Resonant Band Gap. J Appl Mech 2006;73(1):167–70.
[78] Wang G, Yu D, Wen J, Liu Y, Wen X. One-dimensional phononic crystals with locally resonant structures. Phys Lett A 2004;327(5–6):512–21.
[79] Milton GW, Willis JR. On modifications of Newton's second law and linear continuum elastodynamics. Proc Royal Soc A: Mathem, Phys Eng Sci. 2007;463(2079):855–880.
[80] Goffaux C, Sanchez-Dehesa J, Yeyati AL, Lambin P, Khelif A, Vasseur JO, et al. Evidence of fano-like interference phenomena in locally resonant materials. Phys Rev Lett 2002;88(22):225502.
[81] Mitchell SJ, Pandolfi A, Ortiz M. Effect of Brittle Fracture in a Metaconcrete Slab under Shock Loading. J Eng Mech 2016;142(4):4016010.
[82] Sugino C, Xia Y, Leadenham S, Ruzzene M, Erturk A. A general theory for bandgap estimation in locally resonant metastructures. J Sound Vib 2017;406:104–23.
[83] Yao S, Zhou X, Hu G. Investigation of the negative-mass behaviors occurring below a cut-off frequency. New J Phys 2010;12(10):103025.
[84] Yao S, Zhou X, Hu G. Experimental study on negative effective mass in a 1D mass–spring system. New J Phys 2008;10(4):043020.
[85] Huang HH, Sun CT. Anomalous wave propagation in a one-dimensional acoustic metamaterial having simultaneously negative mass density and Young's modulus. J Acoust Soc Am 2012;132(4):2887–95.
[86] Wang T, Sheng M-P, Qin Q-H. Multi-flexural band gaps in an Euler-Bernoulli beam with lateral local resonators. Phys Lett A 2016;380(4):525–9.
[87] Fang N, Xi D, Xu J, Ambati M, Srituravanich W, Sun C, et al. Ultrasonic metamaterials with negative modulus. Nat Mater 2006;5(6):452–6.
[88] Ma G, Sheng P. Acoustic metamaterials: From local resonances to broad horizons. Sci Adv 2016;2(2):e1501595.
[89] Kelkar PU, Kim HS, Cho KH, Kwak JY, Kang CY, Song HC. Cellular Auxetic Structures for Mechanical Metamaterials: A Review. Sensors (Basel) 2020;20(11):3132.
[90] Zhu R, Liu XN, Hu GK, Sun CT, Huang GL. A chiral elastic metamaterial beam for broadband vibration suppression. J Sound Vib 2014;333(10):2759–73.
[91] Liu Y, An X, Chen H, Fan H. Vibration attenuation of finite-size metaconcrete: Mechanism, prediction and verification. Compos A Appl Sci Manuf 2021;143:106294.
[92] Xu C, Chen W, Hao H. The influence of design parameters of engineered aggregate in metaconcrete on bandgap region. J Mech Phys Solids 2020;139:103929.
[93] Hajjaj MM, Tu J. A seismic metamaterial concept with very short resonators using depleted uranium. Arch Appl Mech 2021;91(5):2279–300.
[94] Yan Y, Cheng Z, Menq F, Mo YL, Tang Y, Shi Z. Three dimensional periodic foundations for base seismic isolation. Smart Mater Struct 2015;24(7):75006–11.
[95] Yan Y, Laskar A, Cheng Z, Menq F, Tang Y, Mo YL, et al. Seismic isolation of two dimensional periodic foundations. J Appl Phys 2014;116(4):44908.
[96] Xu C, Chen W, Hao H, Bi K, Pham TM. Experimental and numerical assessment of stress wave attenuation of metaconcrete rods subjected to impulsive loads. Int J Impact Eng 2022;159:104052.
[97] Jin H, Hao H, Chen W, Xu C. Spall Behaviors of Metaconcrete: 3D Meso-Scale Modelling. Int J Struct Stab Dyn 2021;21(09):2150121.
[98] Mitchell SJ, Pandolfi A, Ortiz M. Investigation of elastic wave transmission in a metaconcrete slab. Mech Mater 2015;91:295–303.
[99] Briccola D, Cuni M, De Juli A, Ortiz M, Pandolfi A. Experimental Validation of the Attenuation Properties in the Sonic Range of Metaconcrete Containing Two Types of Resonant Inclusions. Exp Mech 2020;61(3):515–32.
[100] Jin H, Hao H, Chen W, Xu C. Influence of Bandgap on the Response of Periodic Metaconcrete Rod Structure under Blast Load. J Mater Civ Eng 2022;34(11):04022284.
[101] Xu C, Chen W, Hao H, Pham TM, Bi K. Damping properties and dynamic responses of metaconcrete beam structures subjected to transverse loading. Constr Build Mater 2021;311:125273.

[102] Xu C, Chen W, Hao H, Jin H. Effect of engineered aggregate configuration and design on stress wave attenuation of metaconcrete rod structure. Int J Solids Struct 2021;232:111182.
[103] Huang HH, Sun CT. Wave attenuation mechanism in an acoustic metamaterial with negative effective mass density. New J Phys 2009;11(1):013003.
[104] Huang HH, Sun CT. A study of band-gap phenomena of two locally resonant acoustic metamaterials. Proc Inst Mech Eng, Part N: J Nanoeng Nanosyst 2011; 224(3):83–92.
[105] Tan KT, Huang HH, Sun CT. Optimizing the band gap of effective mass negativity in acoustic metamaterials. Appl Phys Lett 2012;101(24):241902.
[106] Khan MH, Li B, Tan KT. Impact load wave transmission in elastic metamaterials. Int J Impact Eng. 2018;118:50–59.
[107] Liu S-f, Chen H-l, Liu Y, He H-g, An X-y, Jin F-n, Fan H-l. Vibration attenuation of meta-mortar with spring-mass resonators. Defence Technol. 2023;20:11–23.
[108] Calius EP, Bremaud X, Smith B, Hall A. Negative mass sound shielding structures: Early results. physica status solidi (b). 2009;246(9):2089–2097.
[109] Manimala JM, Sun CT. Microstructural design studies for locally dissipative acoustic metamaterials. J Appl Phys 2014;115(2):023518.
[110] An X, Lai C, Fan H, Zhang C. 3D acoustic metamaterial-based mechanical metalattice structures for low-frequency and broadband vibration attenuation. International Journal of Solids and Structures. 2020;191-192:293–306.
[111] Cho S, Kim B, Min D, Park J. Tunable two-dimensional acoustic meta-structure composed of funnel-shaped unit cells with multi-band negative acoustic property. J Appl Phys 2015;118(16):163103.
[112] Rong J, Ye W. Topology optimization design scheme for broadband non-resonant hyperbolic elastic metamaterials. Comput Methods Appl Mech Eng. 2019;344: 819–836.
[113] Chen Y, Qian F, Zuo L, Scarpa F, Wang L. Broadband and multiband vibration mitigation in lattice metamaterials with sinusoidally-shaped ligaments. Extreme Mechanics Letters. 2017;17:24–32.
[114] Hu J, Yu TX, Yin S, Xu J. Low-speed impact mitigation of recoverable DNA-inspired double helical metamaterials. Int J Mech Sci. 2019;161-162:105050.
[115] Li Z, Hu H, Wang X. A new two-dimensional elastic metamaterial system with multiple local resonances. Int J Mech Sci. 2018;149:273–284.
[116] Bückmann T, Kadic M, Schittny R, Wegener M. Mechanical metamaterials with anisotropic and negative effective mass-density tensor made from one constituent material. physica status solidi (b). 2015;252(7):1671–1674.
[117] Baravelli E, Ruzzene M. Internally resonating lattices for bandgap generation and low-frequency vibration control. J Sound Vib 2013;332(25):6562–79.
[118] Li H, Li Y, Li J. Negative stiffness devices for vibration isolation applications: A review. Adv Struct Eng 2020;23(8):1739–55.
[119] Lin S, Zhang Y, Liang Y, Liu Y, Liu C, Yang Z. Bandgap characteristics and wave attenuation of metamaterials based on negative-stiffness dynamic vibration absorbers. Journal of Sound and Vibration. 2021;502:116088.
[120] Su YC, Sun CT. Design of double negativity elastic metamaterial. Int J Smart Nano Mater 2015;6(1):61–72.
[121] Chen H, Li XP, Chen YY, Huang GL. Wave propagation and absorption of sandwich beams containing interior dissipative multi-resonators. Ultrasonics. 2017;76:99–108.
[122] Chen JS, Sharma B, Sun CT. Dynamic behaviour of sandwich structure containing spring-mass resonators. Compos Struct 2011;93(8):2120–5.
[123] Jin H, Hao H, Hao Y, Chen W. Predicting the response of locally resonant concrete structure under blast load. Construction and Building Materials. 2020;252: 118920.
[124] Jin H, Hao H, Chen W, Xu C. Effect of enhanced coating layer on the bandgap characteristics and response of metaconcrete. Mech Adv Mater Struct 2021;30(1): 175–88.
[125] Briccola D, Ortiz M, Pandolfi A. Experimental validation of metaconcrete blast mitigation properties. J Appl Mech 2017;84(3):031001.
[126] Briccola D, Tomasin M, Netti T, Pandolfi A. The Influence of a Lattice-Like Pattern of Inclusions on the Attenuation Properties of Metaconcrete. Front Mater. 2019;6.
[127] Xu C, Chen W, Hao H, Pham TM, Li Z, Jin H. Dynamic compressive properties of metaconcrete material. Constr Build Mater. 2022;351:128974.
[128] Xu C, Chen W, Hao H, Pham TM, Bi K. Static mechanical properties and stress wave attenuation of metaconcrete subjected to impulsive loading. Eng Struct. 2022;263:114382.
[129] Lee SH, Park CM, Seo YM, Wang ZG, Kim CK. Acoustic metamaterial with negative density. Phys Lett A 2009;373(48):4464–9.
[130] Vo NH, Pham TM, Bi K, Hao H. Model for analytical investigation on meta-lattice truss for low-frequency spatial wave manipulation. Wave Motion. 2021;103: 102735.
[131] Vo NH, Pham TM, Bi K, Chen W, Hao H. Stress Wave Mitigation Properties of Dual-meta Panels against Blast Loads. Int J Impact Eng. 2021;154:103877.
[132] Kim S-H, Das MP. Artificial Seismic Shadow Zone by Acoustic Metamaterials. Mod Phys Lett B 2013;27(20).
[133] Witarto W, Wang SJ, Yang CY, Nie X, Mo YL, Chang KC, et al. Seismic isolation of small modular reactors using metamaterials. AIP Adv 2018;8(4):045307.
[134] Achaoui Y, Ungureanu B, Enoch S, Brûlé S, Guenneau S. Seismic waves damping with arrays of inertial resonators. Extreme Mech Lett. 2016;8:30–37.
[135] Brule S, Javelaud EH, Enoch S, Guenneau S. Experiments on seismic metamaterials: molding surface waves. Phys Rev Lett 2014;112(13):133901.
[136] Meng L, Cheng Z, Shi Z. Vibration mitigation in saturated soil by periodic pile barriers. Comput Geotechn. 2020;117:103251.
[137] Palermo A, Krodel S, Marzani A, Daraio C. Engineered metabarrier as shield from seismic surface waves. Sci Rep. 2016;6:39356.
[138] Palermo A, Vitali M, Marzani A. Metabarriers with multi-mass locally resonating units for broad band Rayleigh waves attenuation. Soil Dynam Earthq Eng. 2018; 113:265–277.
[139] Colombi A, Roux P, Guenneau S, Gueguen P, Craster RV. Forests as a natural seismic metamaterial: Rayleigh wave bandgaps induced by local resonances. Sci Rep 2016;6(1):19238.
[140] Finocchio G, Casablanca O, Ricciardi G, Alibrandi U, Garescì F, Chiappini M, et al. Seismic metamaterials based on isochronous mechanical oscillators. Appl Phys Lett 2014;104(19):191903.
[141] Colombi A, Colquitt D, Roux P, Guenneau S, Craster RV. A seismic metamaterial: The resonant metawedge. Sci Rep 2016;6(1):27717.
[142] Zeng Y, Xu Y, Yang H, Muzamil M, Xu R, Deng K, Peng P, Du Q. A Matryoshka-like seismic metamaterial with wide band-gap characteristics. International Journal of Solids and Structures. 2020;185-186:334–341.
[143] Elford DP, Chalmers L, Kusmartsev FV, Swallowe GM. Matryoshka locally resonant sonic crystal. J Acoust Soc Am 2011;130(5):2746–55.
[144] Shi Z, Cheng Z, Xiang H. Seismic isolation foundations with effective attenuation zones. Soil Dynam Earthq Eng. 2014;57:143–151.
[145] Xiang HJ, Shi ZF, Wang SJ, Mo YL. Periodic materials-based vibration attenuation in layered foundations: experimental validation. Smart Mater Struct 2012;21(11): 112003.
[146] Jia G, Shi Z. A new seismic isolation system and its feasibility study. Earthq Eng Eng Vib 2013;9(1):75–82.
[147] La Salandra V, Wenzel M, Bursi OS, Carta G, Movchan AB. Conception of a 3D Metamaterial-Based Foundation for Static and Seismic Protection of Fuel Storage Tanks. Front Mater. 2017;4.
[148] Zhou W, Bi K, Hao H, Pham TM, Chen W. Development of locally resonant meta-basement for seismic induced vibration control of high-rise buildings. Eng Struct. 2023;275:115229.
[149] Li Q, Yang D. Mechanical and Acoustic Performance of Sandwich Panels With Hybrid Cellular Cores. J Vib Acoust 2018;140(6):061016.
[150] Li Z, Chen W, Hao H. Crushing behaviours of folded kirigami structure with square dome shape. Int J Impact Eng. 2018;115:94–105.
[151] Lam L, Chen W, Hao H, Li Z, Ha NS. Dynamic crushing performance of bio-inspired sandwich structures with beetle forewing cores. Int J Impact Eng 2022; 173:104456.
[152] Clough EC, Ensberg J, Eckel ZC, Ro CJ, Schaedler TA. Mechanical performance of hollow tetrahedral truss cores. Int J Solids Struct 2016;91:115–26.
[153] Hammetter CI, Rinaldi RG, Zok FW. Pyramidal lattice structures for high strength and energy absorption. J Appl Mech 2013;80(4):041015.
[154] Chen JS, Sun CT. Dynamic behavior of a sandwich beam with internal resonators. J Sandw Struct Mater 2011;13(4):391–408.
[155] Sharma B, Sun CT. Impact load mitigation in sandwich beams using local resonators. J Sandw Struct Mater 2015;18(1):50–64.
[156] Yu D, Liu Y, Zhao H, Wang G, Qiu J. Flexural vibration band gaps in Euler-Bernoulli beams with locally resonant structures with two degrees of freedom. Phys Rev B 2006;73(6):064301.
[157] Yu D, Liu Y, Wang G, Zhao H, Qiu J. Flexural vibration band gaps in Timoshenko beams with locally resonant structures. J Appl Phys 2006;100(12):124901.
[158] Liu Y, Yu D, Li L, Zhao H, Wen J, Wen X. Design guidelines for flexural wave attenuation of slender beams with local resonators. Phys Lett A 2007;362(5–6): 344–7.
[159] Ding L, Ye Z, Wu Q-Y. Flexural vibration band gaps in periodic Timoshenko beams with oscillators in series resting on flexible supports. Adv Struct Eng 2020;23(14): 3117–27.
[160] Wang T, Sheng M-P, Guo Z-W, Qin Q-H. Flexural wave suppression by an acoustic metamaterial plate. Appl Acoust 2016;114:118–24.
[161] Fang X, Wen J, Bonello B, Yin J, Yu D. Ultra-low and ultra-broad-band nonlinear acoustic metamaterials. Nat Commun 2017;8(1):1288.
[162] Cheng Z, Shi Z, Mo YL, Xiang H. Locally resonant periodic structures with low-frequency band gaps. J Appl Phys 2013;114(3):33532.
[163] Manimala JM, Sun CT. Numerical investigation of amplitude-dependent dynamic response in acoustic metamaterials with nonlinear oscillators. J Acoust Soc Am 2016;139(6):3365.
[164] Yilmaz C, Hulbert GM, Kikuchi N. Phononic band gaps induced by inertial amplification in periodic media. Phys Rev B 2007;76(5):054309.
[165] Banerjee A, Adhikari S, Hussein MI. Inertial amplification band-gap generation by coupling a levered mass with a locally resonant mass. Int J Mech Sci 2021;207: 106630.
[166] Li J, Li S. Generating ultra wide low-frequency gap for transverse wave isolation via inertial amplification effects. Phys Lett A 2018;382(5):241–7.
[167] Taniker S, Yilmaz C. Design, analysis and experimental investigation of three-dimensional structures with inertial amplification induced vibration stop bands. Int J Solids Struct 2015;72:88–97.
[168] Kulkarni PP, Manimala JM. Longitudinal elastic wave propagation characteristics of inertant acoustic metamaterials. J Appl Phys 2016;119(24):245101.
[169] Hussein MI, Frazier MJ. Metadamping: An emergent phenomenon in dissipative metamaterials. J Sound Vib 2013;332(20):4767–74.
[170] Chen YY, Barnhart MV, Chen JK, Hu GK, Sun CT, Huang GL. Dissipative elastic metamaterials for broadband wave mitigation at subwavelength scale. Compos Struct 2016;136:358–71.
[171] Barnhart MV, Xu X, Chen Y, Zhang S, Song J, Huang G. Experimental demonstration of a dissipative multi-resonator metamaterial for broadband elastic wave attenuation. J Sound Vib 2019;438:1–12.
[172] Banerjee A, Das R, Calius EP. Frequency graded 1D metamaterials: A study on the attenuation bands. J Appl Phys 2017;122(7):75101.

[173] Huang GL, Sun CT. Band Gaps in a Multiresonator Acoustic Metamaterial. J Vib Acoust 2010;132(3):031003.
[174] Xiao Y, Wen J, Wen X. Broadband locally resonant beams containing multiple periodic arrays of attached resonators. Phys Lett A 2012;376(16):1384–90.
[175] Ho KM, Cheng CK, Yang Z, Zhang XX, Sheng P. Broadband locally resonant sonic shields. Appl Phys Lett 2003;83(26):5566–8.
[176] Zhi-Ming L, Sheng-Liang Y, Xun Z. Ultrawide Bandgap Locally Resonant Sonic Materials. Chin Phys Lett 2005;22(12):3107–10.
[177] Yang Z, Dai HM, Chan NH, Ma GC, Sheng P. Acoustic metamaterial panels for sound attenuation in the 50–1000 Hz regime. Appl Phys Lett 2010;96(4):041906.
[178] Banerjee A, Das R, Calius EP. Vibration transmission through an impacting mass-in-mass unit, an analytical investigation. Int J Non Linear Mech 2017;90:137–46.
[179] Banerjee A, Calius EP, Das R. An impact based mass-in-mass unit as a building block of wideband nonlinear resonating metamaterial. Int J Non Linear Mech 2018;101:8–15.
[180] Banerjee A, Calius EP, Das R. Impact based wideband nonlinear resonating metamaterial chain. Int J Non Linear Mech 2018;103:138–44.
[181] Lou J, Fang X, Du J, Wu H. Propagation of fundamental and third harmonics along a nonlinear seismic metasurface. Int J Mech Sci 2022;221:107189.
[182] Lou J, Fang X, Fan H, Du J. A nonlinear seismic metamaterial lying on layered soils. Eng Struct 2022;272:115032.
[183] Zhang S, Lou J, Fan H, Du J. A nonlinear acoustic metamaterial beam with tunable flexural wave band gaps. Eng Struct 2023;276:115379.
[184] Bonanomi L, Theocharis G, Daraio C. Wave propagation in granular chains with local resonances. Phys Rev E Stat Nonlin Soft Matter Phys 2015;91(3):033208.
[185] Banerjee A, Sethi M, Manna B. Vibration transmission through the frictional mass-in-mass metamaterial: An analytical investigation. Int J Non Linear Mech 2022;144:104035.
[186] Alamri S, Li B, Tan KT. Dynamic load mitigation using dissipative elastic metamaterials with multiple Maxwell-type oscillators. J Appl Phys 2018;123(9):095111.
[187] Xu X, Barnhart MV, Fang X, Wen J, Chen Y, Huang G. A nonlinear dissipative elastic metamaterial for broadband wave mitigation. Int J Mech Sci 2019;164:105159.
[188] Fang X, Lou J, Chen YM, Wang J, Xu M, Chuang K-C. Broadband Rayleigh wave attenuation utilizing an inertant seismic metamaterial. Int J Mech Sci 2023;247:108182.
[189] Smith MC. Synthesis of mechanical networks: the inerter. IEEE Trans Autom Control 2002;47(10):1648–62.
[190] Papageorgiou C, Houghton NE, Smith MC. Experimental Testing and Analysis of Inerter Devices. J Dyn Syst Meas Contr 2009;131(1).
[191] Smith MC. The Inerter: A Retrospective. Ann Rev Control, Robot, Autonomous Syst 2020;3(1):361–91.
[192] Wang FC, Hong MF, Chen CW. Building suspensions with inerters. Proc Inst Mech Eng C J Mech Eng Sci 2009;224(8):1605–16.
[193] Ma R, Bi K, Hao H. Inerter-based structural vibration control: A state-of-the-art review. Eng Struct 2021;243:112655.
[194] Chen MZQ, Hu Y, Huang L, Chen G. Influence of inerter on natural frequencies of vibration systems. J Sound Vib 2014;333(7):1874–87.
[195] Hu Y, Chen MZQ, Smith MC. Natural frequency assignment for mass-chain systems with inerters. Mech Syst Signal Process. 2018;108:126–139.
[196] Al Ba'ba'a H, DePauw D, Singh T, Nouh M. Dispersion transitions and pole-zero characteristics of finite inertially amplified acoustic metamaterials. J Appl Phys 2018;123(10):105106.
[197] Cacciola P, Tombari A, Giaralis A. An inerter-equipped vibrating barrier for noninvasive motion control of seismically excited structures. Struct Control Health Monit 2019;27(3):e2474.
[198] Sun F, Xiao L, Bursi OS. Optimal design and novel configuration of a locally resonant periodic foundation (LRPF) for seismic protection of fuel storage tanks. Eng Struct 2019;189:147–56.
[199] Zhang L, Wang K, Shu H, Wang L, Wang X. New metamaterial foundation based on novel omnidirectional high-performance inerter mechanism. Phys Status Solidi (b) 2023;260(4).
[200] Fang X, Chuang K-C, Jin X-L, Wang D-F, Huang Z-L. An inertant elastic metamaterial plate with extra wide low-frequency flexural band gaps. J Appl Mech 2021;88(2):021002.
[201] Jin X, Chen MZQ, Huang Z. Minimization of the beam response using inerter-based passive vibration control configurations. Int J Mech Sci 2016;119:80–7.
[202] Dong Z, Chronopoulos D, Yang J. Enhancement of wave damping for metamaterial beam structures with embedded inerter-based configurations. Appl Acoust 2021;178:108013.
[203] Xiao Y, Wen J, Wen X. Flexural wave band gaps in locally resonant thin plates with periodically attached spring–mass resonators. J Phys D Appl Phys 2012;45(19). pp. 195401–195401-195412.
[204] Lou J, He L, Yang J, Kitipornchai S, Wu H. Wave propagation in viscoelastic phononic crystal rods with internal resonators. Appl Acoust 2018;141:382–92.
[205] Krushynska AO, Miniaci M, Bosia F, Pugno NM. Coupling local resonance with Bragg band gaps in single-phase mechanical metamaterials. Extreme Mech Lett. 2017;12:30–36.
[206] Matlack KH, Bauhofer A, Krodel S, Palermo A, Daraio C. Composite 3D-printed metastructures for low-frequency and broadband vibration absorption. Proc Natl Acad Sci USA 2016;113(30):8386–90.